Lunds Universitets Naturgeografiska Institution

Seminarieuppsatser Nr. 59

Analysing land cover changes in the Caprivi Strip, Namibia, using Landsat TM and Spot XS imagery.

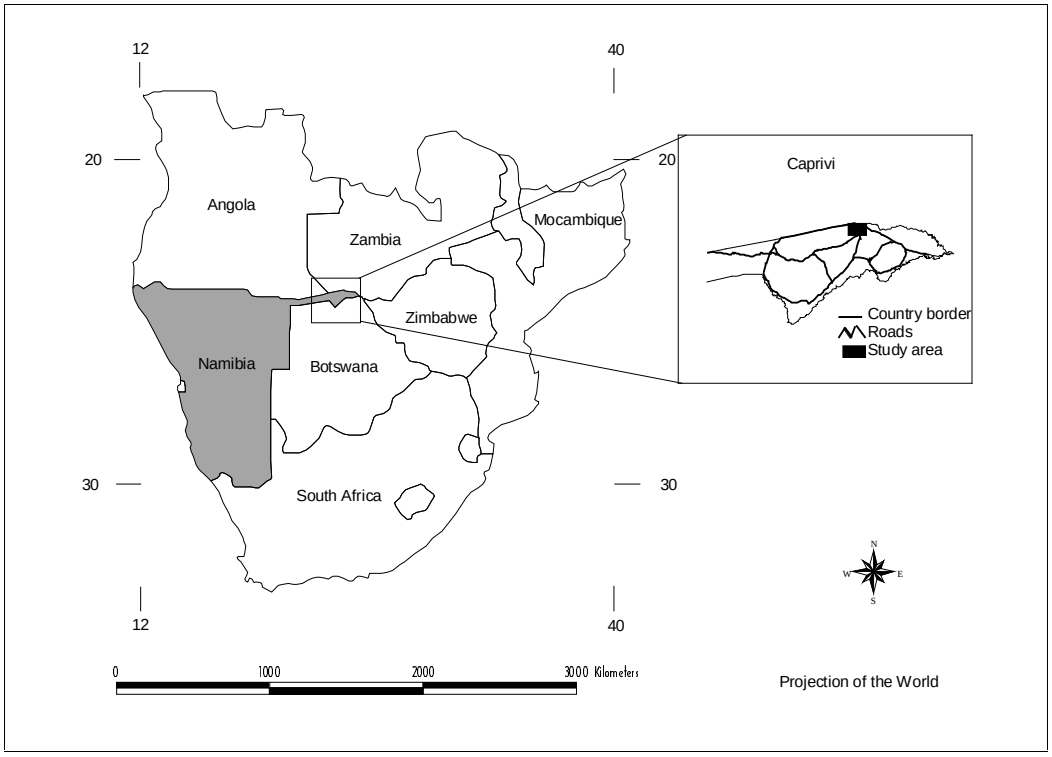

Lisa Hallgren och Anna Johansson

Department of Physical Geography,
Lund University
Sölvegatan 13, S-221 00 Lund,
Sweden

1999

TABLE OF CONTENTS

ABSTRACT

The Caprivi area, situated in the north-eastern part of Namibia, Africa, has experienced a high population increase during the latest ten years. Studies have shown that the vegetation has been influenced as the woodlands, that provide the population with timber and charcoal, have been cut down. Also, the fires have increased in the area, as the people need to cultivate the land in a higher degree. Since the country is widespread, remote sensing is an alternative to field studies in order to survey the extent of vegetation changes.

It was suggested by the NRSC (National Remote Sensing Centre) in Namibia, that a vegetation change method in the area was to be studied. The method should be swift and yet accurate. Using two different satellite scenes, one SPOT XS from 1992 and one Landsat TM from 1994, a method analysing signatures with a paired t-test was used. Three spectral band were examined, the green, the red and the near infrared, in each scene. Together with a signature separability test, the t-test showed if changes had occurred or not in each band and which signatures that were separable. Using literature studies, the result was analysed and interpreted. Both the vegetation change method and precipitation data from the area showed that the climatic conditions has become drier during the time period, as the green vegetation cover has decreased and become more senesced. The short time duration did not prove any substantial human influence on the tree cover.

ACKNOWLEDGEMENTS

We would like to express our gratitude to the people working at the Department of Physical Geography at Lund University. They have all been very helpful. A warm thanks to our supervisor, PhD Lennart Olsson, who helped and guided us whenever it was necessary. We would also like to thank PhD Jonas Ardö for supporting us with literature and knowledge.

Further, we would like to thank our supervisor in Namibia, Mr Harold Kisting at the NRSC who provided us with the satellite scenes, precipitation data and the vegetation and the soil classification. We also thank the staff at the NRSC for helping us with their computer systems.

The study has been financed by SIDA, without whose contribution this study could not have been carried out. A special thanks to Mrs Monica Halling at the SLU in Uppsala, who granted the scholarship.

Andreas. Thank you for being there.

1 INTRODUCTION

The Caprivi region in the north-eastern part of Namibia, Africa, is experiencing a high population increase. A recent forest inventory made by the National Remote Sensing Centre (NRSC), Windhoek, Namibia, showed swift changes of vegetation in the Caprivi strip.

A hundred years ago 6000 people lived in the Caprivi area, about 20000 km^2 in size. The present population is about 18 times higher. When Namibia became independent in 1990, the pressure on the environment started to grow rapidly. The forest vegetation cover has decreased by an average of 0.3% annually from 1990 to 1997 due to an increased cultivation since the area became more secure in the early 1990's (esa, 1990; NRSC, 1998).

During contacts between PhD Lennart Olsson, Department of Physical Geography, Lund, and Mr Harold Kisting, NRSC, Namibia, it was suggested that a vegetation change detection method for the area ought to be studied. To finance the study an application was written to SIDA (Swedish International Development Agency) in order to apply for a scholarship. SIDA participates in international development and its main task is to promote development in their partner countries. The SIDA program for MFS (Minor Field Study) is a scholarship for Swedish university students to seek knowledge about developing countries. Students can apply for a scholarship in order to carry out a field study abroad during at least two months.

To develop a method, based on digital satellite data and remote sensing technology, satellite and ground based evaluation data from the area were acquired. Contacts with staff at the NRSC before the journey resulted in information that they had two Landsat TM scenes that should be used in the study, one from 1994 and one from 1997. Later it proved that they had one SPOT scene from 1992 and one Landsat TM from 1994, which should be used. Preparation for the fieldwork was done in Sweden, before the journey, and at the NRSC office in Windhoek. NRSC helped to choose a study area that consisted of both cultivated and uncultivated land and was close to a relatively large city. The closeness to the city was important due to that the increasing population living there would affect the land more noticeably and it was easier to rent a room. There was also a matter of safety since the Unita guerrilla had been spotted along the Angolan border. The NRSC provided data management assistance, satellite scenes purchased from SSC (Swedish Space Corporation), Sweden and transportation to the field study site. A local helped to determine the different tree species in the area.

1.1 Aim

The main purpose of this study is to use a change detection method for vegetation, based on remote sensing. The method does not require a classification of scenes resulting in thematic maps, but uses variance analysis of spectral signatures in the two satellite scenes. The aim is also to compare and prepare the original scenes in

order to carry out the variance analysis. The following three components are the main structure of the study.

- Correct and compare a SPOT XS to a Landsat TM scene
- Determine if variance analysis of the spectral signatures from the scenes, combined with a separability analysis, could be used in order to make a land cover change detection
- Determine if there had been a change of vegetation during 1992 and 1994

Difficulties were expected in correcting the SPOT to the Landsat TM scene since they have different spectral resolutions and because of that the SPOT scene was saturated. The authors assumed that there had been only a minor change of vegetation due to the short time period. However, scars caused by fire ought to affect the area since forest fires have increased during the 1990's. Also, we expected changes in the edge of the woodlands and nearby inhabited areas.

1.2 Background

The forest is an important natural resource in developing countries. It provides the population with timber and charcoal and it also prevents soil degradation and erosion. The land cover change is due to both natural and human causes although the human is the major influence. The most important natural effects are drought and bush fire. Bush fires caused by humans have increased due to changes in traditional agriculture methods and an increasing population. The number of people in the area keeps growing fast and causes increasing pressure on the environment (esa, 1991). In the southern part of Africa problems arise from the pressure of human and livestock population. Development activities like increasing water usage, tourism pressure and demands of arable land affects the wildlife and causes various forms of land degradation. The effect of heavy grazing leads both to decreases in the cover density and biodiversity (Ringrose *et al*., 1997).

Compared with other parts of Namibia, the Caprivi Strip contains relatively dense forests and woodlands and the pressure on these are high due to increasing population. It is therefore important to evaluate the woodland cover regularly to prevent further land degradation before it is a fact. For long-term regional, national and local planning it is important with both qualitative and quantitative forest information which is needed for forest management and for the assessment and monitoring of forest resources (esa, 1991).

1.3 Study area

1.3.1 Location of the area

The satellite data used in this study covers an area of longitude 24°08´42´´ to 24°32´25´´ E, latitude 17°43´31´´ to 17°62´57´´ S (Figure 1), with the town Katima Mulilo in the north. The area is situated in the Caprivi region in the north east of

Namibia, Africa. The field study in the area was carried out the first week of September 1998.

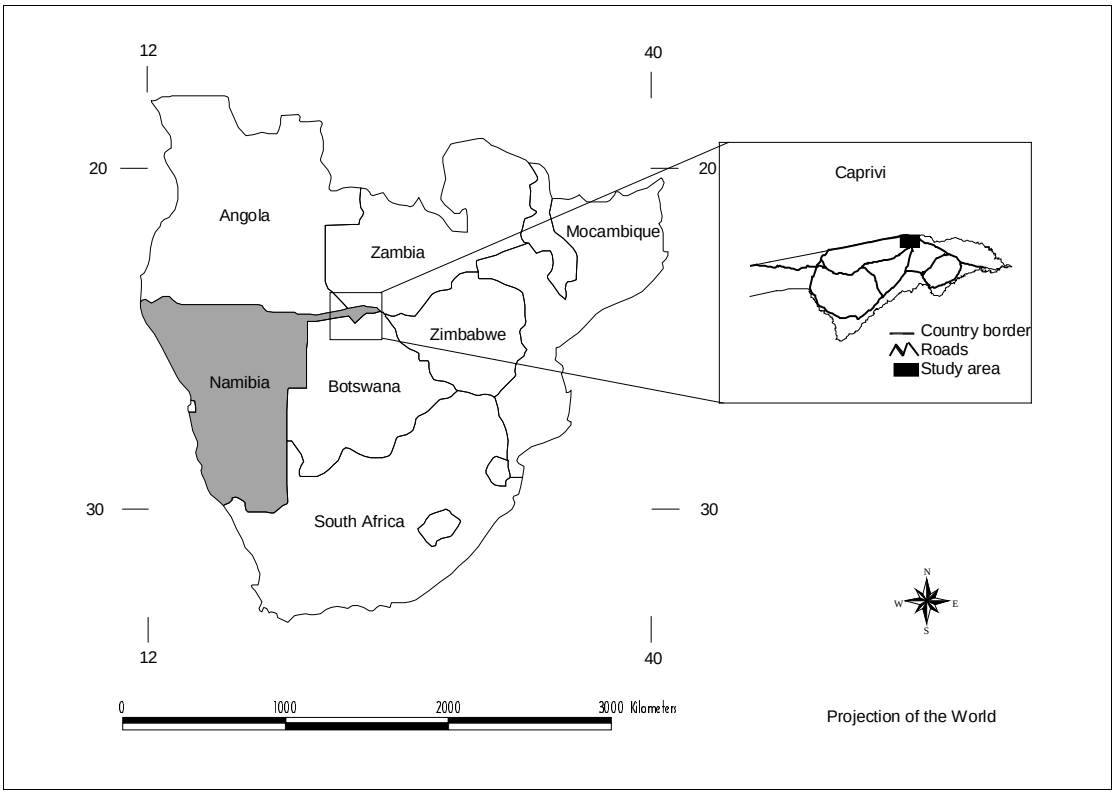

***Figure 1**. The study area (the black rectangle) is situated in the north-eastern part of Namibia, Africa.*

1.3.2 Topography

Topographically, Caprivi is flat without a single feature recognisable as a hill. The elevation gradually drops from 1100 m above sea level in the west to 930 m in the east. The elevation in the study area ranges from 960 to 980 m (ONC P-4, 1989).

1.3.3 Geology and vegetation

The geology consists mainly of ancient erosion surfaces with acid crystalline igneous rocks, aeolian sands and sandstone. The soil has a high iron oxide content which makes its colour reddish (Scholes, 1997). Close to the Zambesi river the soil is more brownish and consists of calcareous material. The study area is covered with thick deposits of fossil, parallel Kalahari sand dunes except along certain sections of the river courses. The height of the dunes in the study area are of little importance, but in the whole Caprivi they could be as high as 30 m.

The vegetation in Caprivi is generally some form of woody grassland referred to as savanna (Cowling & Hilton-Taylor, 1997). In Caprivi, moist savannas often change gradually into woodlands and open semi-decidous forests. They are often being maintained as savannas by clearing and agriculture, but most of all by fires. The forests along the rivers are often evergreens, due to the enhanced moist status. A savanna have at least a two layered above ground structure: a tree layer with a discontinuous crown cover, 2-10 m tall, that overlies a grassy layer, 0.5-2 m tall. An

intermediate layer of small trees or shrubs is sometimes present. Savannas can be subdivided on the basis of height and tree canopy of the tree layer; mainly shrublands and woodlands (Scholes, 1997).

The vegetation in the study area was divided into 8 major land cover types (Figure 2), mainly according to a vegetation map made by the NRSC (Vegetation map, 1997):

- Open grassland
- Grassland
- Shrubland
- Mopane woodland
- Burkea woodland
- Teak woodland
- River woodland
- Cultivated area

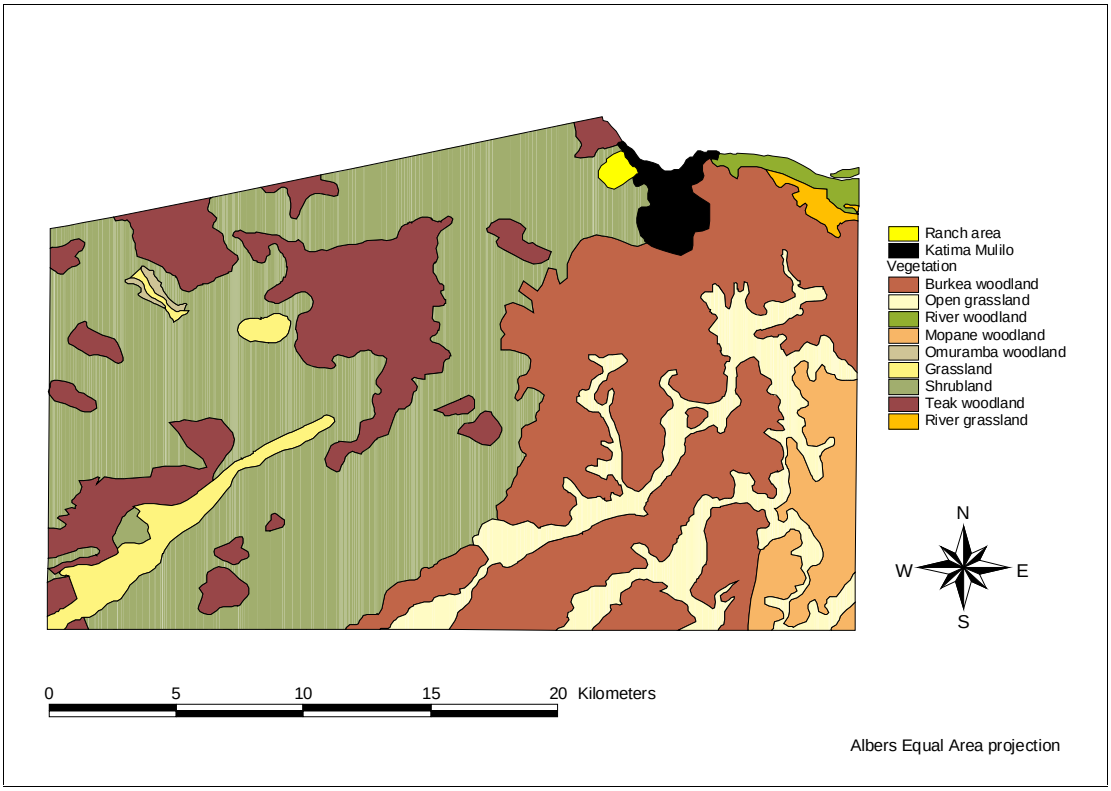

Figure 2. *Vegetation types in the study area,modified from map made by NRSC (Vegetation Map, 1997).*

The open grassland is situated on clay loam soil and has moderate vegetation coverage. A denser grass cover is found in the grassland in the western part of the study area. It is situated on a sandy loam and is experiencing a high livestock population. The shrubland is covered with both higher trees, bushes and grass, and the soil is sandy. This soil type is also found in the Teak woodland and in the Burkea woodland, where the trees are high and stands relatively close. The Mopane woodland consists of tall trees, situated on clay loam. The river woodland contains a 15 – 20 m corridor of evergreen forests along the river and then a mixture of mainly Mopane and Acacia species (Soil Map, 1997; Scholes, 1997; van Wyk & van Wyk, 1995).

The cultivated areas are usually small, but the ranch area (Figure 2) consists of irrigated cultivated land.

1.3.4 Climate

Even though Namibia often is characterised as hot and dry, the Caprivi strip is distinctly more tropical. It has higher rainfall, less evaporation and a warmer winter than the rest of the country (Schulze, 1997). The rainfall is highly variable from year to year and from one place to another which induces serious droughts from time to time, the latest taking place during the 1990's.

Almost all of Caprivi´s rain falls during the summer months September to May. In September and October small falls may occur but it is only in November that there is enough rain to start growing crops. The precipitation usually peaks in January and February with as much as 160 mm rainfall (Figure 3). The average rainfall in the study area is between 600 - 700 mm/year but has been generally lower in recent years (Windhoek Weather Bureau, 1997). During the period August 1991 to July 1992, the annually rainfall was 568 mm. For August 1992 to July 1993, it was 623 mm and for the period August 1993 to July 1994, it was 501 mm.

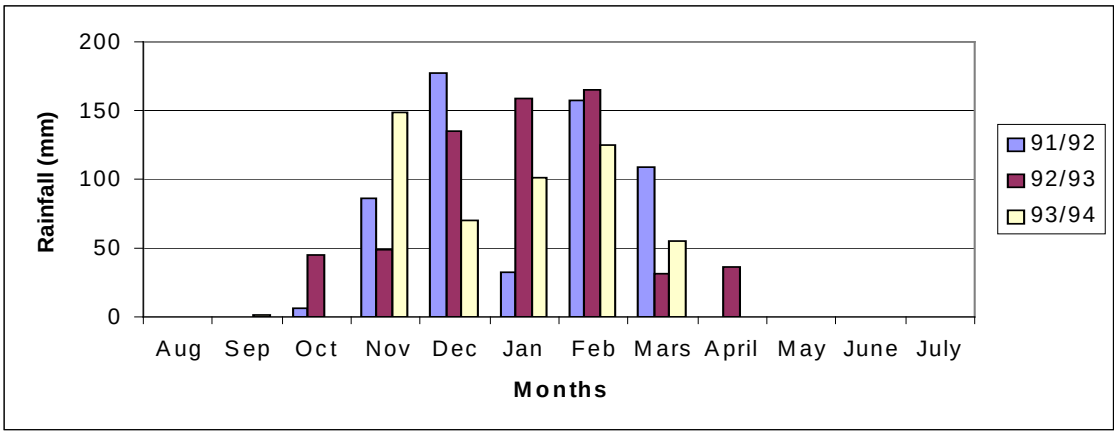

Figure 3. *The average precipitation in Katima Mulilo during 1992 to 1994 (Windhoek Weather Bureau, 1997).*

The highest temperatures in the study area occur in September to November when the cloud cover is low. The average daily maximums are between 32 and 35° C. Average daily minimum temperatures vary between 20° C in summer and 5° C in winter. The evaporation rate is highest in September and October (Windhoek Weather Bureau, 1997).

2 THEORETICAL BACKGROUND

This section is mainly a theoretical background to the sensors and the imaging processing methods that was used in the study. First, there is a brief discussion about the Landsat TM, SPOT and NOAA AVHRR sensors used in the study. Then the geometric and radiometric calibration is discussed together with the difference between SPOT XS and Landsat TM sensors and how they could be compared and equalised. Also, the NDVI and the Fourier analysis used on the AVHRR time series are explained and then, the different spectral signatures found in the area and their characteristics in each spectral band. In the end, the separability test and variance analysis and how they can be used in vegetation change studies are discussed.

2.1 Satellite sensors

Different satellite sensors operate in different spectral wavelengths and with different resolutions. Each sensor has its own characteristics which affects the resulting digital numbers (DN) in an image. These characteristics must be considered in order to be able to accomplish an accurate evaluation of the data. Since the aim is to compare image data from two sensing systems it is important to have knowledge about their similarities and differences.

2.1.1 SPOT sensor

The French satellites SPOT 1 and 2 (Systeme Probatoire d´Óbservation de la Terre), launched in 1986 and 1990 respectively, carries two identical imaging devices known as HRV´s. The HRV is often referred to as a ”push-broom” scanner, where each detector in the array scans a strip across the track direction. Since it also has a long effective dwell time for each pixel, a high spatial resolution is possible (Lillesand & Kiefer, 1979). The SPOT satellite provides two imaging modes, one multispectral (Table 1) called XS and one panchromatic, named PAN.

Table 1. *HRV characteristics in the multispectral mode (Richards, 1986).*

HRV:	**Spectral bands:**	0.50 - 0.59 μm (green)
		0.61 - 0.68 μm (red)
		0.79 - 0.89 μm (near infrared)
	Ground resolution:	20 x 20 m

The two HRV instruments are mounted side by side which makes the satellite able to operate parallel, perpendicular or each angled up to 27° from the vertical line. The large angle of the sensors makes it possible for the satellite to cover the same area on the Earth with an interval of one to five days only (Schott, 1997).

2.1.2 Landsat TM sensor

The Landsat earth resource system started in 1972 with the launch of Landsat 1. The first satellite carried two imaging instruments; RBV (Return Beam Videcon) and MSS (Multi Spectral Scanner). In 1982, Landsat 4 was launched carrying the first

TM (Thematic Mapper) sensor. The Thematic Mapper is a mechanical scanning device that acquires data by scanning the Earth's surface in strips normal to the satellite motion. Six lines are swept simultaneously by an oscillating mirror and the wavelength bands of the satellite detect the reflected solar radiation. The TM has an improved spectral, spatial and radiometric characteristics compared to the MSS (Richards, 1986; Schott, 1997). Seven wavelength bands are used (Table 2).

Table 2. *Landsat TM sensor characteristics (Richards, 1986, Schott, 1997).*

TM:	**Spectral bands:**	0.45 - 0.52 μm (blue)
		0.52 - 0.60 μm (green)
		0.63 - 0.69 μm (red)
		0.76 - 0.90 μm (near infrared)
		1.55 - 1.75 μm (middle infrared)
		10.4 - 12.5 μm (thermal infrared)
		2.08 - 2.35 μm (middle infrared)
	Ground resolution:	30 x 30 m (band 6: 120 x 120 m)

2.1.3 NOAA AVHRR sensor

The NOAA (National Oceanographic and Atmospheric Administration) AVHRR (Advanced Very High Resolution Radiometer) has been designed to provide information for hydrologic, oceanographic and meteorological studies (Lillesand & Kiefer, 1979; Richards, 1986). The nadir resolution of the system, 1.1 km, becomes coarser increasing in view angle off-nadir that may be as high as 8 km (Schott, 1997). The AVHRR sensor uses five wavelength bands (Table 3).

Table 3*. NOAA AVHRR sensor characteristics (Richards, 1986).*

AVHRR:	**Spectral bands:**	0.58 – 0.68 μm (red)
		0.72 – 1.1 μm (near infrared)
		3.55 – 3.93 μm (middle infrared)
		10.3 – 11.3μm (thermal infrared)
		11.5 – 12.5 μm(thermal infrared)
	Ground resolution:	1100 x 1100 m

Compared to SPOT XS and Landsat TM, NOAA satellites have a very low spatial resolution. This compensates by a very good temporal resolution (Richards, 1986; Schott, 1997). NOAA AVHRR is also one of the most widely used time series data for land applications (Olsson & Eklundh, 1994).

2.2 Geometric correction

Satellite scenes have to be system corrected for internal scan distortions (that is, nonlinearity of mirror motion, earth curvature effects, scan skew and sensor altitude variations). This is usually done at the receiving stations, since specific data about the satellite is required (Muller 1993).

System corrected TM and SPOT data have a good geometric quality which allows geodetic rectifications to subpixel precision. Two different satellite scenes may be geometrically corrected to each other using GCP's (Ground Control Points) consisting of stable objects such as large buildings, road intersections, river bends and piers (Richards, 1986; Hill & Aifadopoulou, 1990). GCP's are chosen, in both scenes, in order to perform a resampling that corrects one scene to another. The resampling accuracy of the GCP's is reported as a root mean square (RMS) error. It reports the standard deviation of differences between actual values of GCP's and their calculated values (Campbell, 1996). The RMS error is normally set to below 0.5 pixels in order to carry out a resampling. Different resampling algorithms can be used in the process; nearest neighbour, cubic convolution and bilinear interpolation.

Most suitable, if classification follows the registration or if subtle variations in the grey levels need to be retained, is the nearest neighbour interpolation since it does not alter the original grey level value, but simply rearranges its position. It determines the grey level from the closest pixel to the specified input coordinates and assigns that value to the output coordinates (Richards, 1986). The most complex but probably the most widely used resampling method is cubic convolution. It uses a weighted average of values within a neighbourhood of adjacent pixels. This method is used if it is important for the pixels to be placed exactly above each other (Richards, 1986; Campbell, 1996).

2.3 Radiometric correction

When a satellite sensor records image data, it may contain errors in the measured values of the pixel. It is generally assumed that ground objects always have a specific spectral signature. However, these signatures are dependent on different factors such as sensor characteristics, sun-target-satellite geometry, date of acquisition, atmospheric parameters and local environment (Richards, 1986; Muller, 1993).

The radiometric effects on the image data can be divided into two categories:

- Sensor related effects
- Scene related effects

The sensor related effects may be divided into absolute and relative calibration (Pilesjö, 1992). An absolute radiometric calibration is usually not possible for the user to accomplish, as it involves optic, climatic and atmospheric parameters. It is normally performed at the receiving stations.

The usual approach consists in a relative calibration of data (Price, 1987; Hill & Aifadopoulous, 1990). Raw digital numbers are converted to spectral radiance ($mW/cm^2/sr/\mu m$). Then, the data usually is corrected for scene related effects. These are sun angle and irradiance variations, atmospheric effects and topographic effects. In order to correct for the sun angle and the irradiance variations, a common method is to recalculate the spectral radiance into at-satellite reflectance. The reflectance values are then re-scaled to 8 bit data ranging from 0-255. All bands are scaled using

the same constants in order to retain the inter-band relationship. This is important if the scene is to be compared with another scene.

Equation (1) is used in conversions from absolutely calibrated digital numbers to spectral radiance ($mW/cm^2/sr/\mu m$) for Landsat MSS and Landsat TM. Data used in the equation is valid for Landsat-4 and Landsat-5 (Campbell, 1996 from Markham & Barker, 1986).

$$L_\lambda = (DN/DN_{max}) \times (L_{max} - L_{min}) + L_{min} \quad (1)$$

L_λ = spectral radiance ($mW/cm^2/sr/\mu m$)
DN = the specific digital number from the scene in a given band
DN_{max} = maximum digital number for a given sensor
L_{min} = the sensors minimum brightness
L_{max} = the sensors maximum brightness

The conversion from spectral radiance to at-satellite reflectance corrects for differences in sun angle and solar irradiance equation (2) (Price 1987).

$$\rho p_\lambda = (\pi \times L_\lambda \times d^2) / (Esun_\lambda \times \cos\Theta) \quad (2)$$

ρp_λ = unitless at-satellite reflectance
d = earth-sun distance in astronomical units
$Esun_\lambda$ = mean solar exoatmospheric spectral irradiance in ($mW/ cm^2/sr$)
Θ = solar zenith angle

Atmospheric effects, caused by scattering and absorbing effects of the atmosphere, may be removed from the signal using different methods (Richards, 1986). One is to assume that the longest waveband is essentially unaffected by atmospheric scattering and the minimum DN value in this band are subtracted from all pixel values in all bands (Ahlcrona, 1988). Another approach is to use stable areas, i.e., areas that are assumed to have non-changing spectral properties. One dark area, such as water, and one bright area, preferably soil with no vegetation or moisture differences, in each scene is used to stretch the images linearly. Water bodies should have a brightness value at very near zero in the infrared portion of the spectrum since water absorbs strongly and little infrared energy is scattered to the sensor (Campbell, 1996). Soil usually has a high brightness value.

Studies of the topographical effect in terrain dominated by gentle slopes only shows that the relationship between topographic parameters and variations in spectral radiance was weak for forests and cultivated land cover classes. The Landsat response analysed was not found to be related to terrain parameters and it is concluded that the effect of topography is of little importance in cultivated fields (Hall-Könyves, 1988).

2.4 Correcting SPOT to Landsat TM

When a SPOT XS and a Landsat TM scene is to be compared, the SPOT XS is almost always corrected to the Landsat TM if necessary. This is due to the better spectral response of the Landsat TM sensor. Classifications of vegetation show that Landsat TM agreements were approximately 4 percent higher than SPOT using a supervised approach (Joria *et al.*, 1991). This mostly depends on that when comparing SPOT channels XS 1-2-3 and Landsat TM channels 2-3-4, which are spectrally most similar, it shows that the latter gives a higher spectral separability because of the width and the placement of the spectral bands (Büttner & Csillag, 1989).

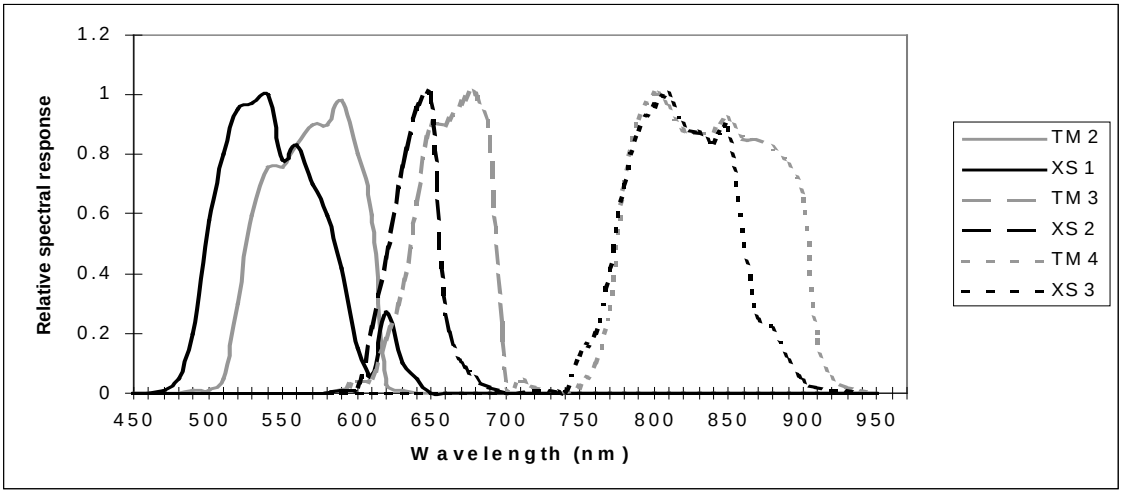

Figure 4. *The relative spectral response of Landsat TM 2-3-4 and SPOT XS 1-2-3 (Guyot & Gu, 1994).*

As presented in Figure 4, the relative spectral response of the sensor SPOT-1 and Landsat-5 TM are different. Homologous spectral bands do not coincide and are centered on different wavelengths (Table 4). Since the radiance of an object varies with wavelengths, differences in the measured equivalent radiances are induced. For example, vegetation targets will have a larger radiance in TM 2-3 than in corresponding XS 1-2, but will be practically equal in the near infrared band (Guyot & Gu, 1994).

Table 4. *The difference of the homologous spectral bands TM 2-3-4 and XS 1-2-3 (Richards, 1986).*

	Wavelength (μm)		
Sensor	**Green**	**Red**	**Near infrared**
SPOT XS:	0.50 – 0.59	0.61 – 0.68	0.79 – 0.89
Landsat TM:	0.52 – 0.60	0.63 – 0.69	0.76 – 0.90

There are several different methods for correcting the two sensors to each other. According to Muller (1993), the spectral sensitivities of SPOT and TM bands may be considered as almost equivalent, even though they are not strictly the same, and be adjusted by simple translations (e.g., normalisation method). However, some differences between the data still persist in some land cover classes. The method implies that raw data are normalised using image based parameters such as unchanging areas. Their mean radiometric value is used to create a regression equation that was applied on the scenes. Muller concluded in his article that the

normalisation method gave a better result than did correcting the two scenes radiometrically to at-satellite reflectance and then carry out an atmospheric correction.

Hall-Könyves (1988) found that a standardisation method could be used in order to compare two different satellite scenes. This method implies that the image containing the smallest reflectance value of an unchanging area may be used as a standard and be subtracted from the reflectance values of this target in the same band of the other dates. Due to the uncertainty of the unchanging areas, the standardisation procedure should be based on the mean value of all unchanging areas used.

Problems exist when spectral changes are analysed with different sensors since the effect of sensor and angular factors on the spectral signatures on the ground objects cannot be quantified accurately unless images are acquired simultaneously. This is not achievable in practice. Also, atmospheric and *in situ* ground measurements are necessary (Hall-Könyves, 1988). Using atmospheric measurements to calibrate the sensors in order to characterise the mean spectral effect for a pair of homologous channels, a proportionally constant may be determined. This enables conversion of the data from one sensor to those of another, using equation (3) (Guyot & Gu, 1994).

$$D_i(TM) = a_i * D_i(XS) \quad (3)$$

Where:

D_i = digital number
a_i = proportionally constant

Guyot & Gu (1994) shows that the dynamic range of Landsat TM is smaller than corresponding SPOT XS band in TM2-3 and XS1-2. In the near infrared, the dynamic range of TM is better than XS.

The histogram matching method reassigns digital values in one scene to another scene so that the brightnesses in the output image are equally distributed among the range of output values. This method is often used when improving the appearance of a single band (Campbell, 1996). The procedure uses the cumulative histogram of the source image to obtain new brightness values. It compensates for the detector differences in the scenes since the detectors used in this study gives a different grey level value for the same energy amount (Richards, 1986).

2.5 Normalised Difference Vegetation Index (NDVI)

Various mathematical combinations of the AVHRR channel 1 and 2 have been found to be sensitive indicators of the presence and condition of green vegetation, referred to as vegetation indices. Among the most important of these indices is the NDVI (Lillesand & Kiefer, 1979). The index normalises the difference between the channels and results in a value within -1 and 1 (Tucker, 1979). Vegetated areas will generally yield high values because of the relatively high near-infrared reflectance and low

visible reflectance (Lillesand & Kiefer, 1979). NDVI is calculated according to equation (4):

$$NDVI = (NIR - R) / (NIR + R) \quad (4)$$

Where NIR is the near-infrared reflectance (AVHRR channel 2) and R is the red reflectance (AVHRR channel 1). Channel 1 covers the spectral zone where the green vegetation reflects a minimum of light because chlorophyll absorption, while channel 2 covers the zone where the green vegetation reflection peaks because of the mesophyll (Kennedy, 1989).

2.5.1 Fourier analysis

In order to gather phenological parameters mathematically from a time series, the Fourier analysis is an appropriate method (Olsson & Eklundh, 1994). The analysis is based on an adjustment of trigonometrically functions to a time series. The basic equation used is:

$$f(x) = f(x)mean + \sum_{r=1}^{N/2}\left[a_r \sin(2\pi rx/P) + b_r \cos(2\pi rx/P)\right] \quad (5)$$

Where:

P = the fundamental period of the data
N = the number of observations in the series
r = the harmonic; between 1 and N/2
x = the average of the time series
$f(x)_{mean}$ = the mean of the whole time series

The two Fourier coefficients a_r and b_r are defined according to equation (6) and (7):

$$a_r = 2/N\sum_{x=1}^{N}\left[f(x)\sin(2\pi rx/P)\right] \quad (6)$$

$$b_r = 2/N\sum_{x=1}^{N}\left[f(x)\cos(2\pi rx/P)\right] \quad (7)$$

The Fourier transformation is carried out iteratively, where each harmonic gives a better fit to the original data. The first harmonic has only got one maximum and one minimum while the second harmonic has two maxima and minima and so forth. The higher the harmonic, the higher is the correlation with the original observation. If the study site has a typical mono-modal distribution, the first harmonic will describe it well. The second harmonic will describe a bi-modal distribution.

The Fourier program made by Olsson & Eklundh (1994), calculates the maximum and minimum value of the derivative in the 6th harmonic and when the maximum increase and decrease occurred. When used on a AVHRR NDVI time series, it shows

the increase and decrease of the rainy season since the derivative is used. The program also calculates the modality.

2.6 Spectral signatures

Spectral signature refers to the spectral response of a feature, as observed over a range of wavelengths. Many of the Earth's features have very distinctive spectral reflectance or emmittance curve. The response pattern may be distinctive but not necessarily unique. Factors that can change the spectral response characteristics are temporal effects and spatial effects (Lillesand & Kiefer, 1979). In this section, the spectral response of vegetation during the dry winter season is discussed. The purpose is to supply with a background to the behaviour of spectral signature in different wavelengths.

2.6.1 Green and senesced vegetation

Spectral features of chlorophyll and water dominate the spectrum of green vegetation. Chlorophyll absorbs energy in the wavelength band centred at about 0.45 and 0.65 μm and the reflectance of healthy vegetation increases dramatically at about 0.7 μm. The reflectance in the range of 0.7 to 1.3 μm is highly variable between different plant species due to the internal structure of the plant (Lillesand & Kiefer, 1979).

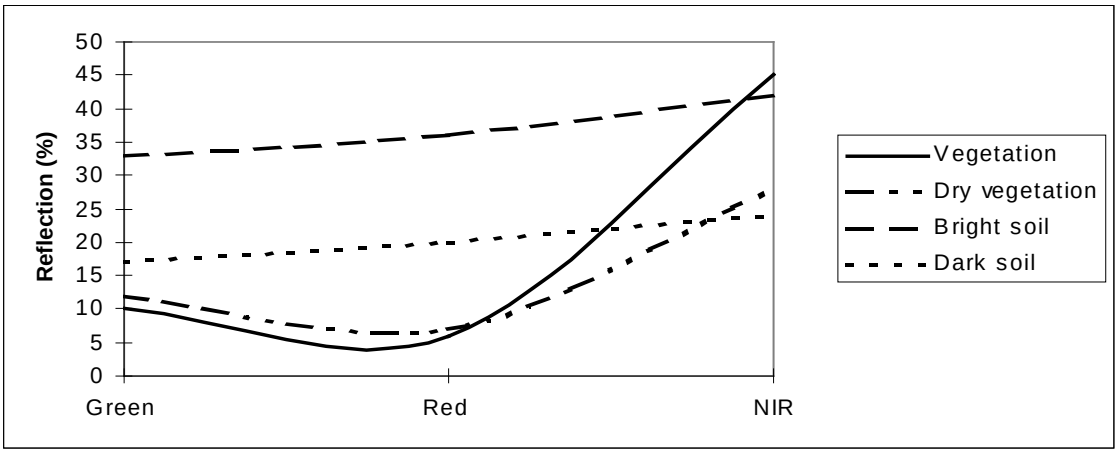

Figure 5. *The reflection spectra of bright and dark soil, vegetation and dry vegetation (Elvidge, 1990; Ringrose et al, 1989).*

In savanna woodland, however, the reflectance in the near infrared region is abnormally low, relative to the amount of green vegetation present (Figure 5). The lower near infrared reflectance depends on the dry climate, the anatomy of the leaves and by high vertical shadows caused by the plant (Ringrose *et al.*, 1989).

When leaves senesces, the chlorophyll starts to break down and as a result, the reflectance in the green and red wavelengths increase. Due to changes and consequent breakdown of the internal structure in the leaves, the reflectance in the NIR wavelengths initially increases and then decreases (Williamson & Eldridge, 1993).

According to Ringrose *et al*. (1997), the average spectral reflectance of woodland and evergreen forests in northern Botswana often shows high near infrared values and low green values. For most classes, the average reflectance of the red band is higher than that of the green band. This is applicable for Teak woodland, Burkea woodland (Figure 6) and river woodland (Figure 7).

Figure 6. *Burkea woodland nearby the town Katima Mulilo in the Caprivi strip.*

Figure 7. *An island in the Zambesi river covered with river woodland*.

2.6.2 Soil

In semiarid areas the soil reflectance is related to thin humus layer, the mineralogy and texture of sands. The precipitated salts on the surface, moisture content and surface roughness are also important factors. Soils with relatively high reflectance appear to have high calcium contents. Even small increments of vegetation tend to darken the soil in the red band and in the NIR, but not as consistently as in the red (Ringrose *et al.*, 1989). Factors that reduce the reflectance are moisture, surface roughness and a high content of organic matter (Lillesand & Kiefer, 1979).

When digital data is collected by satellite sensors, the reflection of vegetation is often mixed with that of soil surface. This may become a problem with vegetation types as shrubland and grassland, where the reflection from vegetation is closely intermingled with the bare soil (Campbell, 1996). Dry, bright soil tends to have a high reflectance

both in the red and the infrared region, but low in the near infrared, compared to living vegetation. Dark soil will show higher reflectance in the green and the red band than does the vegetation, both green and dry (Figure 5). In the near infrared, the soil reflectance is lower than the green vegetation (Ringrose *et al*., 1989). Since the open grassland in the study area consists almost only of bare soil and some senesced vegetation during the winter season, the soil will give a high reflectance in all three wavelengths bands.

2.6.3 Grassland and shrubland

In dry plant material the absorption features occurs in very narrow wavebands (10nm). A large proportion of the pasture is not always photosynthetically active, as it has senesced. Even though soil has higher reflectance than the senesced pasture, the differences in reflectance is not clear due to shadows from vegetation, variations in the soil and cryptogam cover (Williamson & Eldridge, 1993). Dry land, such as grassland (Figure 8) and shrubland (Figure 9), often shows a higher reflectance in the near infrared band than does the woodland.

Figure 8. *An area consisted of open grassland nearby Katima Mulilo.*

Figure 9*. Typical shrubland before rainfall in the Caprivi strip.*

2.6.4 Fire

Burned areas are easily identified because of their low reflectance. The advantage of remote sensing is that it can be used to study the burned vegetation and its following recover. High resolution images can be used to estimate the burned areas. To identify fire scars, TM 4 is the most appropriate since water is not mistaken for fire scars because of the lower grey level. To detect smoke plumes from active fires and smouldering areas, TM 1, 2 and 3 are the best (Pereira & Setzer, 1993).

Fires mostly occur during the periodic dry and hot seasons in Africa. There are quite a lot of different fire types; surface fires, which are most common in savannas and crown fires, which burn the aerial portions of trees and shrubs (Bond, 1997).

2.7 Vegetation change analysis

When carrying out a vegetation change analysis using a variance test, a signature separability analysis is useful. In each satellite scene, the at-satellite reflectance of specific land cover types is extracted for every band and then analysed using a paired t-test. If a land cover type has changed, the separability analysis can be used in order to determine the new type. It is also preferable to have distinctively separated signatures within a scene in order to make the analysis as good as possible.

2.7.1 Battacharrya separability analysis

When a classification of multitemporal and -spectral data is to be performed, a statistic separability test between the classes used may be helpful. Several statistical methods are available to perform this separability analysis, like Battacharrya distance, transformed divergence and Jeffries-Matusita distance. In this study, the Battacharrya distance (BD) measure, based on the Jeffries-Matusita distance will be used, since it is considered to give the best result (Richards, 1986).

The BD measure yields a value between 0 and 2, where 0 indicates complete overlap between the signatures of two areas, and 2 indicates a complete separation.

0.0 – 1.0 very poor separability
1.0 – 1.9 poor separability
1.9 – 2.0 good separability

Very poor separability indicates that the classes are the same. Poor separability that the two signatures are separable to some extent. This is usually caused by large internal variability within the areas (Richards, 1986).

2.7.2 Variance analysis

A fundamental reason that only a few studies have analysed the variance of different satellite scenes is the relative lack of appropriate analytic tools for spatial data. Many techniques are available for analysing remote sensing data, but most require the data to first be classified. A thematic map is easy to evaluate, but much data and information about local pixel variance may be lost in the process (Henebry, 1993). A

simple and yet relatively accurate method of detecting vegetation and land cover change is the variance analysis of spectral signatures. Each land cover type has a distinct spectral signature and by using these, an evaluation of the vegetation may be carried out (Dadhwal *et al.*, 1996).

The signature values of interesting areas in different scenes are extracted and then analysed using a paired t-test. The t-test will show if there has been a change or not in the spectral signature of the area chosen (Dadhwal *et al.*, 1996). The test is unsuitable for a whole satellite scene since it is quite time consuming, but it is applicable for smaller areas and when a user wants to find out if there are any changes in a specific area over time.

The t-test uses parametric data and examines the differences between two samples. It is used when there is a before and an after observation and when the variances of both the observations are necessarily not equal. The test determines if the sample's mean are separable or not. High t-values with little intergroup overlap are a result of a combination between large differences between sample means and with low variances of the samples. Small differences between the two distributions produce smaller t-values having more common statistical ground (Shaw & Wheeler, 1994). That is, a large value indicates a change while a small value indicates no change of vegetation.

3 DATA AND SOFTWARE USED

Different types of data have been used in this study. The main data sets are, one Landsat TM scene, one SPOT XS scene and 36 AVHRR NDVI images. Also, a topographic map (ONC P-4, 1989), a vegetation and soil classification based on the 1994 Landsat TM scene and field studies made by the NRSC (Vegetation Map, 1997; Soil Map, 1997) and precipitation data from the Windhoek Weather Bureau (1997) were used. The accuracy of the vegetation and the soil classification is not known by the authors.

3.1 SPOT and Landsat TM data

Two satellite scenes were primarily used in the study, one SPOT scene from 1992 and one Landsat TM scene from 1994 (Table 5). Both scenes were purchased from SSC, whom also made a geometric correction on both with a RMS error smaller than 1 pixel. The SPOT scene was taken the 22nd of May and the Landsat TM scene the 14th of June.

Table 5. *Information about satellite scenes used.*

Satellite	**Projection**	**Ellipsoid**	**Date**
SPOT-1 XS, HRV 1	Transverse Mercator	Bessel	22/5-1992
Landsat-5 TM	Albers Equal Area	Bessel	14/6-1994

View angles for the SPOT scene was 2.2°, which implies that nadir viewing could be assumed for the radiometric analysis (Hill & Aifadopoulou, 1990).

3.2 NOAA AVHRR data

In order to estimate the phenology of both scenes, NOAA data in GAC-format (Global Area Coverage), with a resolution of 8 km, was collected from the NASA Pathfinder project. The data was stored in Goodes Homolosine Interrupted Projection, which is an equal-area pseudocylindrical map projection. NDVI data were used since it shows the seasonality and phenology very well. The data collected consists of ten day composites that range from August 1991 to July 1994.

3.3 Software used

Different software has been used in the study. For the NDVI data, IDRISI (Eastman 1993), a Fourier program made by Olsson and Eklundh (1994), Vectrans, ProjectV and Goodedir made by Olsson, was used. The SPOT and the Landsat TM data were mainly processed using EASI/PACE (PCI, 1994) and IDRISI. Also, statistic programs, calculation programs and word processing programs was used in the study. Arc View (ESRI, 1996) was used for presentation of most image data and processing of the Digital Chart of the World (DCW, 1992).

4 METHODS

The satellite scenes were first re-projected and geometrically corrected when necessary. Then the Landsat TM was radiometrically corrected and the SPOT scene was corrected according to the sensor differences between them using the Landsat TM as a standard. The Fourier program was used on the NOAA AVHRR data to estimate the rainy period in order to calculate the approximate dates of increase and decrease. Then, the variance of different spectral signatures was calculated and evaluated and a separability analysis was carried out.

4.1 Geometric correction

Both satellite scenes were system corrected by SSC but since they were in different projections, the TM scene was re-projected to Universal Transverse Mercator (UTM) projection, zone 35.

The SPOT scene was geometrically corrected, due to lack of projection data, to the TM scene and resampled using nearest neighbour interpolation to a pixel size of 30 m with a RMS error of less than 0.5 pixel (0.33). Some information was lost in the SPOT scene which was preferred rather than resampling the TM scene to 20 m since it would enhance the data space used. Fifteen unchanging and easily detectable objects (section 2.2) were used as GPC's in the process. Cubic convolution resampling was not used since the variance analysis did not require exactly matching pixels as polygons were used instead of individual pixels (section 2.4).

4.2 Radiometric correction

Each Landsat TM band was radiometrically corrected according to equation (1). The radiance values were then transformed to at-satellite reflectance using equation (2). Measurements of satellite response from stable areas, such as soil, in the TM scene did not indicate any atmospheric effects and since the vegetation in the study area is very flat and comparable with cultivated fields, no atmospheric or topographic correction was made. Water was not used as a stable area since the river was too shallow and no other water bodies were available.

4.2.1 Correcting the satellite bands of TM and XS

To be able to use different sensors for analysing the spectral changes, several methods for correcting the satellite data was tried. The method used was a combination of relative calibration and the normalisation method (Muller, 1993), since it proved to be the most accurate in this case. The SPOT data turned out to be saturated and some soil pixels differed widely from the rest of the pixel values. This made the usual methods unsuitable to use.

Using the at-satellite reflectance corrected Landsat TM data, stable objects were selected. In this case dense woodland and dry grassland was used. Thirty pixel values

were extracted from each band and a regression equation (8) was calculated for each corresponding pair of channels (Table 6).

$$DN_{TM} = \beta_i + \alpha_i DN_{SPOT} \quad (8)$$

***Table 6**. α- and β- constants for correcting SPOT XS to Landsat TM.*

	TM2; XS1	**TM3; XS2**	**TM4; XS3**
α	0.4252	0.529	0.766
β	0.14	10.8	1.81

The SPOT scene was then corrected to fit the Landsat TM scene spectrally, since it was not saturated, had the lowest mean pixel values and no extremes and therefore used as a standard. It's also the most common to correct the SPOT to the Landsat TM scene (section 2.4).

4.3 Fourier analysis

In this study, a Fourier analysis was carried out on time series of AVHRR NDVI data over the Caprivi area. Using the derivative, it was established where the function had extreme values and the rate of change over time in the series (Olsson & Eklundh, 1994). This is useful since the rainy season often starts somewhat before the vegetation starts to grow and ends before the vegetation starts to decrease.

In order to reduce the noise in the data, the 10 day composites was combined to 20 day composites. This was done to minimise the cloud interference in the data, which would disturb the Fourier analysis (Eklundh, 1991).

Since the rainy season in Caprivi lasts during November to April, the year was extended from August to July. The scenes were then examined with the Fourier program to estimate the maximum and minimum increase and decrease of the rainy season. The program also shows if the study area has mono-modal or bi-modal rainy season. A vector file over the study area in Caprivi was created and used to select the exact pixels for the study area in the created Fourier files.

4.4 Vegetation change analysis

The BD measure will be used in order to determine which class a signature belongs to if it has changed during the time period 1992 to 1994. It will also be used to determine if the classes may be spectrally separated before the variance analysis.

In order to carry out a variance analysis over the study area, polygons with varying size and land cover types were digitised in the scenes. These polygons were then used to extract all pixel values represented in each polygon, both from the Landsat TM and the SPOT XS scene. Interesting areas such as the edge of the woodland and highly populated areas in the open grassland, where a change is likely to have taken place, were used. Also areas that were not supposed to have changed at all during the

period, like Teak, Burkea and river woodlands were examined. All resulting spectral signatures were then analysed using a paired t-test in order to find out if they could be separated from each other in time.

The town Katima Mulilo was excluded from the study since the spectral signatures in the town area differed widely from each other, which made the result unreliable. Other minor settlements were to small to give a specific signature, and therefore not used either. Also, uncontrolled and non-irrigated cultivation was to small to be detected by satellite seniors and was excluded as well. The soil pixels containing extreme values in the SPOT scene were neglected from the study, since they were not reliable.

5 RESULTS

5.1 Normalisation method

The unchanging objects were chosen for the stability of their satellite response over time and efforts was made to avoid edge pixels. The resulting pixel values in the corrected SPOT scene corresponded well to the radiometric corrected Landsat TM scene (Figure 10).

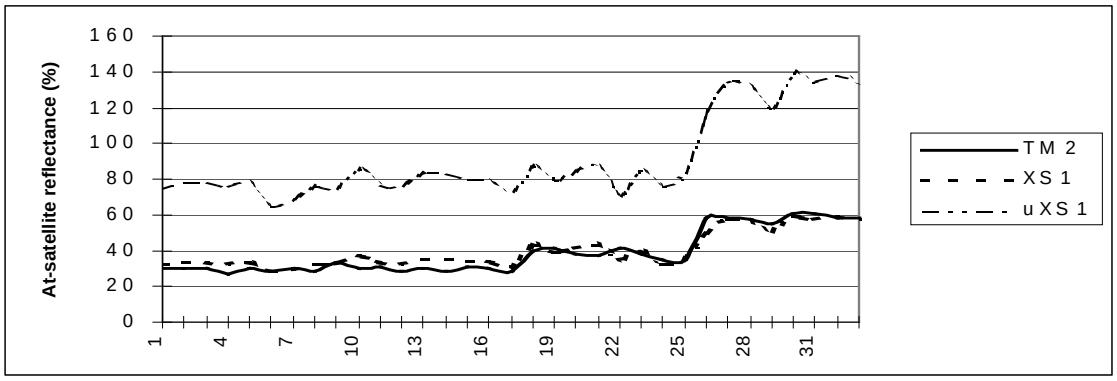

Figure 10. *Comparison of radiometrically corrected TM data (TM2), normalised (XS1) and original (uXS1) SPOT XS data from the green band.*

The normalised SPOT pixel values (XS1) still shows the same fluctuations as the corresponding original SPOT values (uXS1), but they are now comparable with the Landsat TM values (TM2). The first seventeen values consist of Teak woodland, the next eight of Burkea woodland and the last seven of grassland. The two woodlands are almost unseparable in the original SPOT XS1 data, but a slight change is noticed in the Landsat TM and the normalised SPOT. The similarities in at-satellite reflectance of the woodlands in the original SPOT data are due to the saturation in the SPOT scene. Looking at the Teak woodland values, it may be concluded that the values are higher in the normalised SPOT scene than in the Landsat TM scene. This is not detectable in the Burkea woodland or in the grassland.

5.2 Fourier analysis

The Fourier analysis carried out on the AVHRR time series data showed that the rainy seasons during the period August 1991 to July 1994 were quite alike (Table 7). The analysis also showed that the rainy season in the study area was mono-modal.

Table 7*. Approximate date for the beginning and the end of the rainy seasons during the time period August 1992 to July 1994.*

Time period	Day# increase	Approx. date	Day# decrease	Approx. date
1991-1992	114	22/11-1991	245	2/4-1992
1992-1993	93	1/11-1992	251	8/4-1993
1993-1994	103	11/11-1993	259	16/4-1994

The rainy season in 1992 ends the 2nd of April and in 1994, the 16th of April. In 1992, there are 52 days between the maximum decrease in the rainy season and the acquisition date of the satellite scene. In 1994, the difference is 59 days. This indicates that the Landsat TM scene and the SPOT XS scene are comparable according to spectral signature since they were taken in the same part of the vegetation period, that is in the end of the growth season or early winter.

5.3 Battacharrya separability analysis

The separability analysis of the different spectral signature using the Battacharrya distance measure showed that the separability was good between the different classes in both scenes. A common problem with the SPOT sensor is that the class separability is relatively poor compared to Landsat TM, which makes the latter a better choice if a classification is to be carried out, in spite of the better spatial resolution in SPOT. All three bands, the green, the red and the near infrared, were used in each separability analysis, since carrying it out on every single band would give a poor separability. The results of the Battacharrya separability analysis for SPOT and Landsat TM are stored in Appendix I.

5.4 Variance analysis

The paired t-test, used on different vegetation types such as shrubland, grassland, woodland and cultivated areas showed that some changes had occurred. The test is carried out on all three bands in each polygon, which leads to that a signature change may be indicated in one or two bands but not in the others. All polygons were digitised in the Landsat TM scene using the vegetation map from NRSC except for the edge of the wood polygons. These were digitised in the SPOT scene in order to find out if the Teak woodland had expanded or not during the years 1992 to 1994.

The hypothesis of all t-tests is:
H_0 = No signature change has occurred during 1992 to 1994.
H_1 = A signature change has occurred during the period.

T-values larger than approximately 12 leads to a rejection of the H_0 hypothesis, that is, a change has occurred. Usually, the t-values ranges between 0 and 10 if the vegetation type is unchanged and over 20 if a change has occurred. The mean at-satellite reflectance and resulting t-values of all polygons are stored in Appendix II and III. The polygons are numbered from (1) to (27) in order to simplify the reading.

5.4.1 Open grassland and grassland

The polygons (1) to (4) are all situated on open grassland and grassland (Figure 11). The vegetation in polygon (1), consisting of open grassland, has not changed according to the t-test. In polygon (2) and (3) however, the test indicates some changes (Figure 12). The spectral signature in polygon (2) has increased in all bands, while in polygon (3), it has decreased. The increase in (2) is probably due to drought,

as the separability analysis show that the vegetation during the time period has gone from Burkea woodland in 1992 to grassland in 1994. In polygon (3), the reflectance has decreased in each band. The BD measure implies that the area probably has been cultivated since 1992, as the spectral signature resembles those of the cultivated area. The clay loam soil is desirable considering cultivation. The polygon is situated close to the road, which makes easy to reach. It may also indicate a coarser soil texture or a higher content of organic matter than in polygon (2), although it is not as probable.

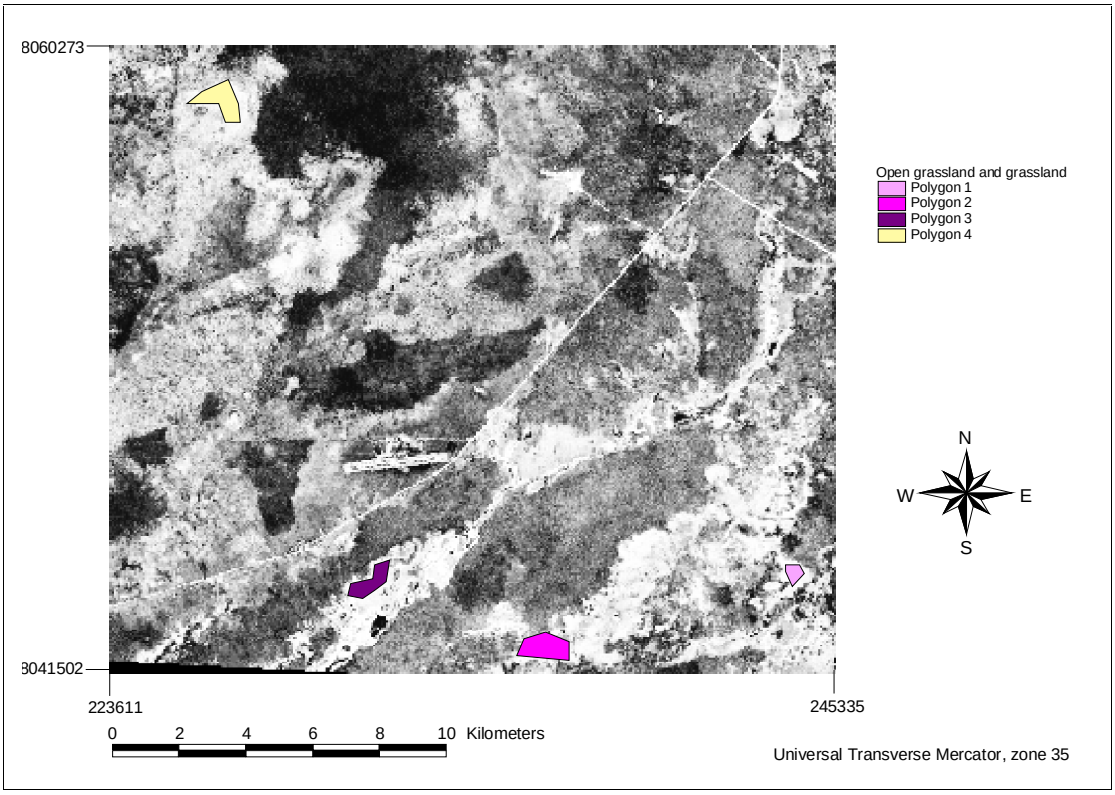

Figure 11. *The open grassland and grassland polygons (1) to (4).*

Polygon (4), consisting of grassland, has changed in the green and the red band according to the t-test. The signature has increased since 1992, which indicates, just like polygon (2), that the soil has become drier. The separability analysis shows that the area either consisted of a more shrubland like vegetation or was cultivated in 1992. The former is more probable as the area is heavily grassed by cattle.

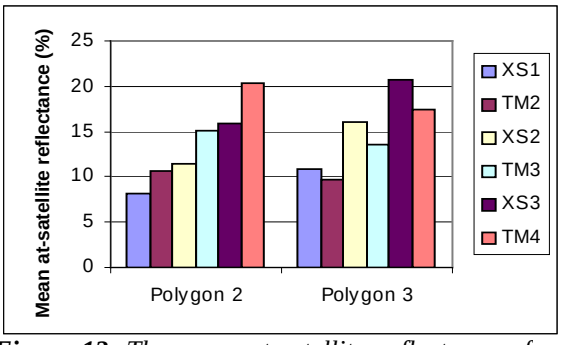

Figure 12. *The mean at-satellite reflectance of open grassland polygon (2) and (3).*

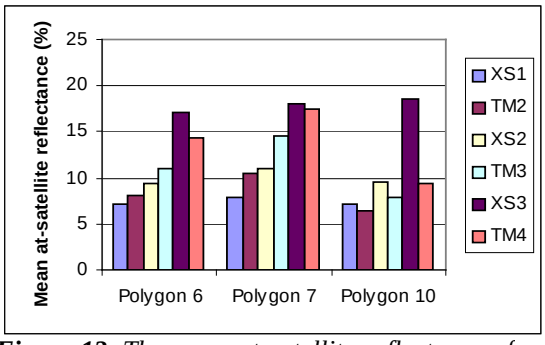

Figure 13. *The mean at-satellite reflectance of shrubland polygons (6), (7) and (10).*

5.4.2 Shrubland

The shrub vegetation in polygons (5) to (8) (Figure 14) has experienced major changes in all three bands, except for the near infrared band in polygon (7) according to the t-test (Figure 13). This is probably due to drought since the mean reflectance has increased in the green and the red band, but decreased in the near infrared. This happens when the vegetation senesces. In polygon (7), the tendency is much weaker and therefore no significant changes can be proved. The BD measure implies no new land cover type.

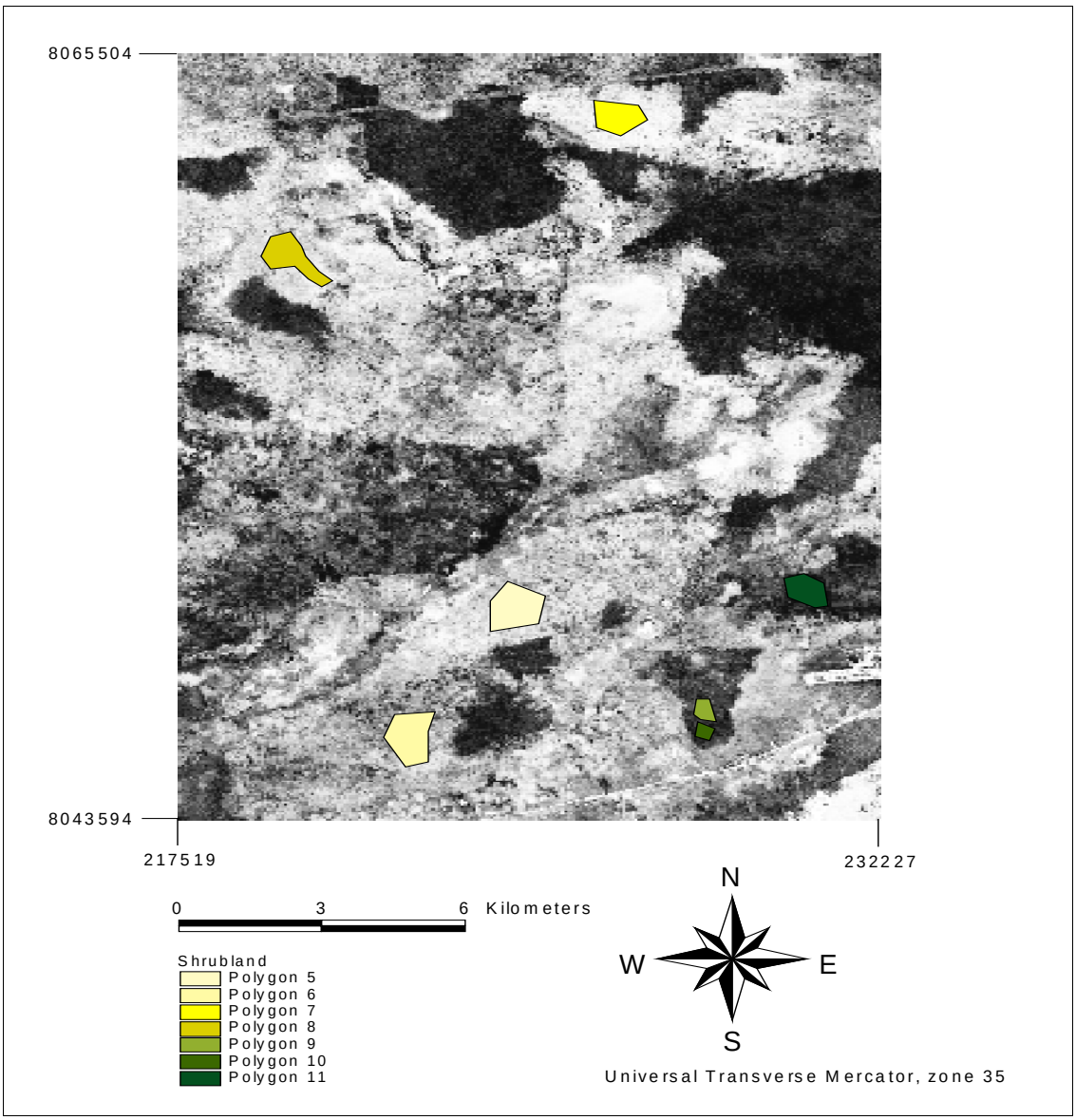

Figure 14. *Polygons (5) to (11) consisting of shrubland.*

In shrubland polygons (9) to (11), the t-values indicate a major change in all the near infrared bands (Figure 13 to 16). This is due to fires in the area, and a change may also be seen in the green and the red band although very small. The separability analysis of the SPOT scene shows that all polygons belong to the same vegetation type. In the TM scene, polygons (9) to (11) differ to (5) to (8) because of the firescars. The fire scars in 1994 (Figure 16) may be due to the drougth, more extensive

cultivation caused by increasing amount of people in the area or a combination of both. No major fire scars are visible in the SPOT scene from 1992 (Figure 15).

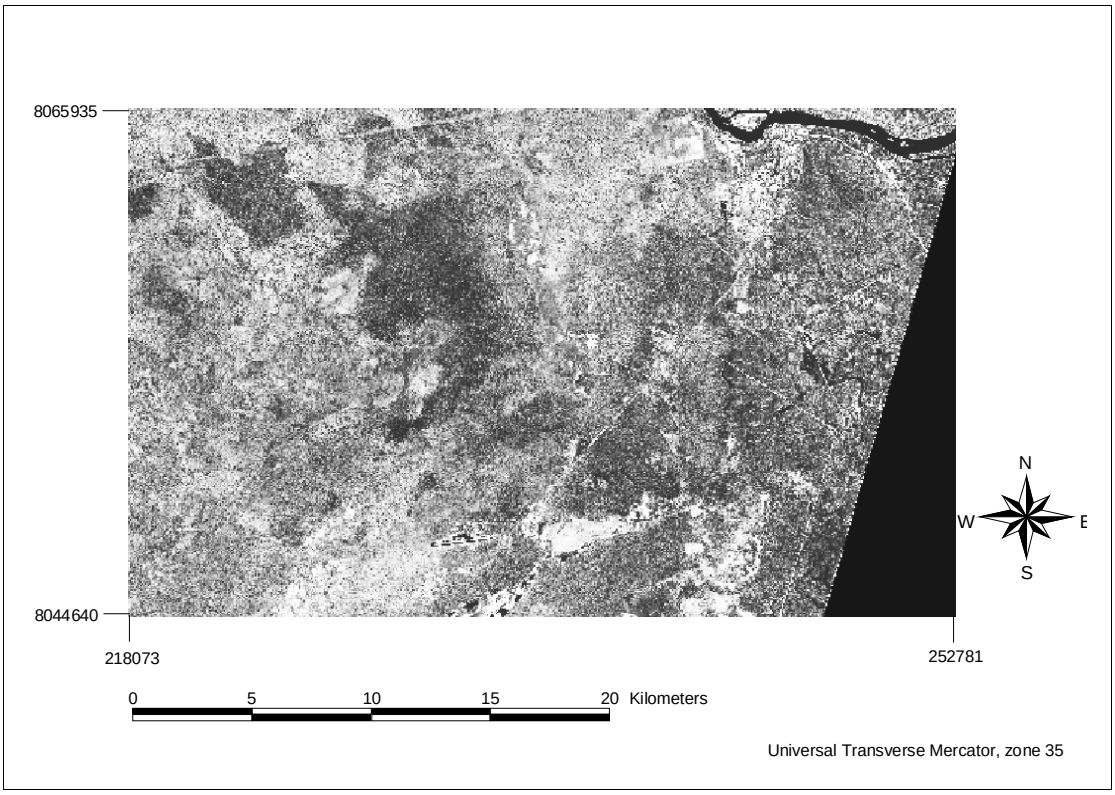

***Figure 15**. The SPOT near infrared band (XS3) shows no sign of major fire scars.*

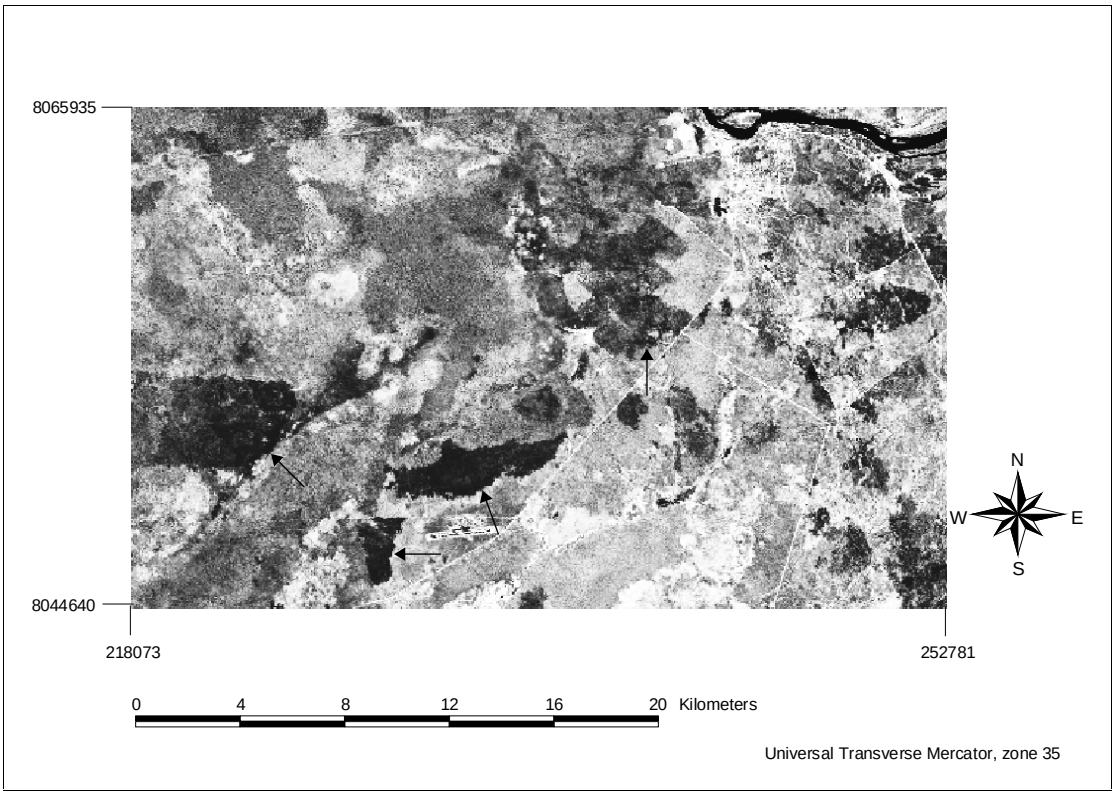

***Figure 16**. In the TM near infrared band (TM4), fire scars appear distinctively (the arrows point out some of the most obvious scars).*

5.4.3 Burkea woodland

The polygons situated in Burkea woodland, (12) to (16) (Figure 17), show no changes according to the t-test. The t-values are low in all three bands in each polygon. The polygons show a very poor separability among each other, but also a poor separability towards the edge of the wood, shrubland and cultivated polygons in both the 1992 and the 1994 scene.

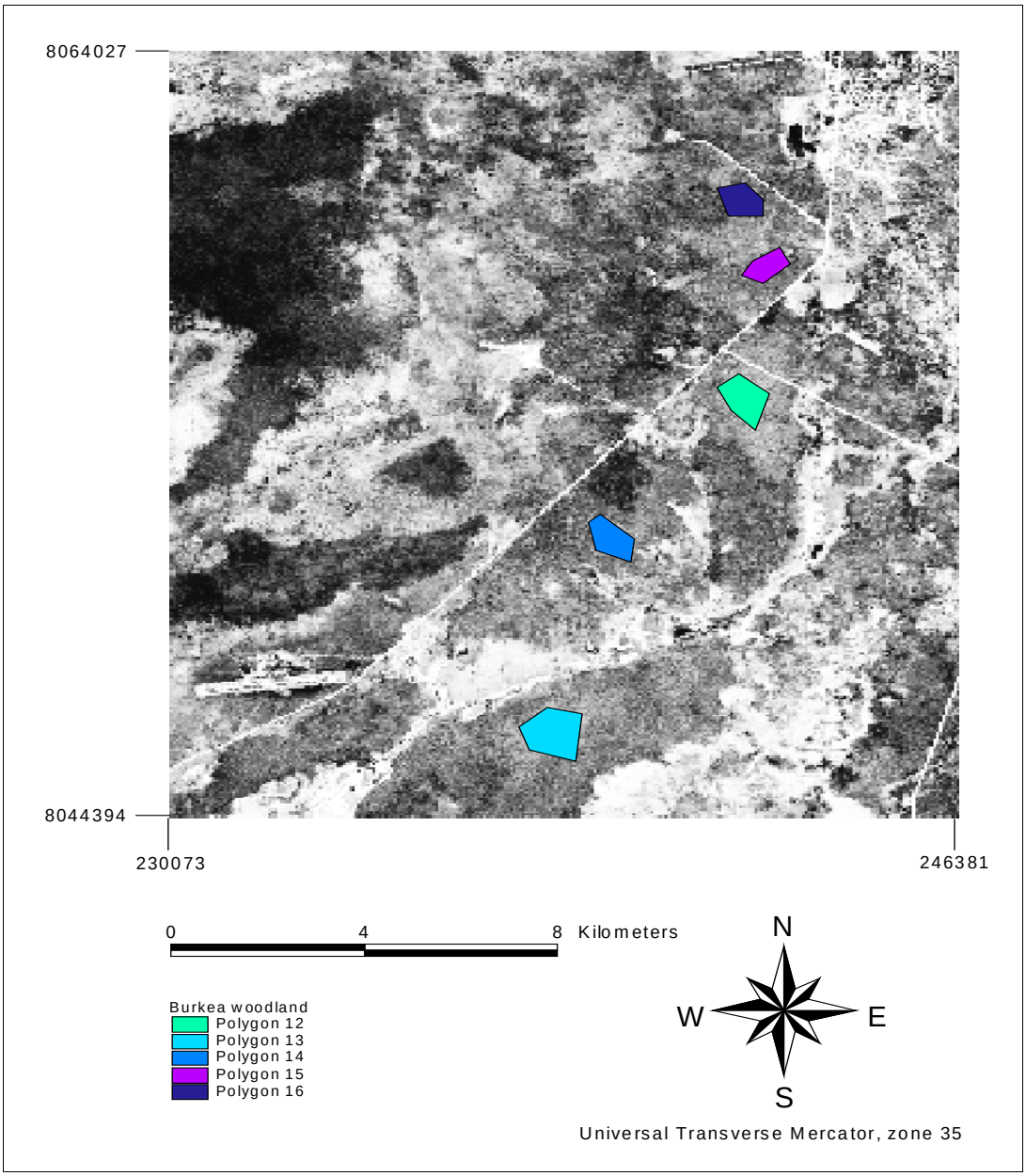

Figure 17. *The Burkea woodland polygons (12) to (16).*

5.4.4 Teak woodland

Polygon (17), (18) and (19) are situated in large stands of Teak woodland (Figure 18). All three polygons show a decrease in the green and the red band. In polygon (17) there has also been a decrease in the near infrared band as well (Figure 20). This may be due to that the trees in the 1992 scene has a smaller amount of senesced leaves

than does the trees in 1994 and may be an indication of drought. The reflectance of the senesced leaves is higher than the signature of the stems and the branches. If the soil had been affecting the signature, the sand would have given a higher reflectance in 1994 than in 1992 because of the drought. The BD measure in both scenes implies that the polygons in the class have similar signatures.

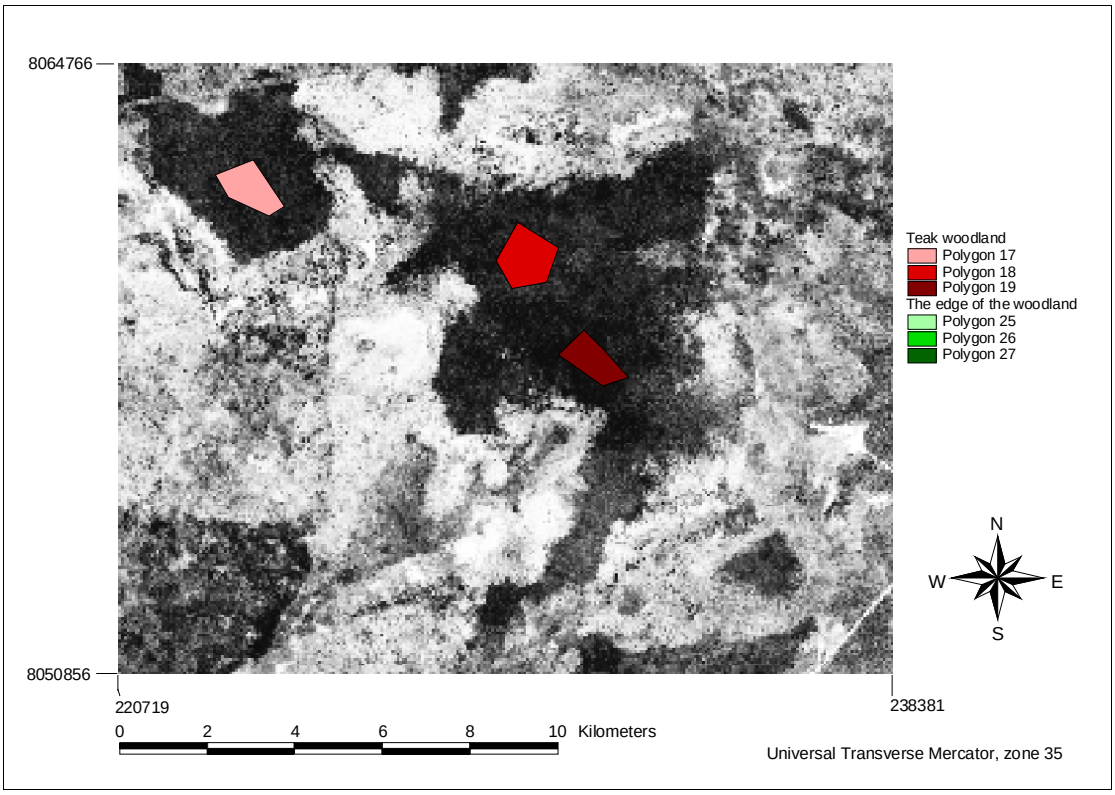

Figure 18. *The teak woodland polygons (17) to (19) and the edge of the wood polygon (25) to (27).*

5.4.5 River woodland

Polygon (20), (21) and (22) consist of river vegetation (Figure 19). However, the result is not all over reliable since the evergreen vegetation is too sparse considering the coarse resolution of the Landsat TM scene. According to the Vegetation map (1997), the river woodland in 1994 has a greater extent of evergreen forest than was proved in field by the authors in 1998. This affects polygon (20), placed by the river on the mainland. The separability analysis shows that the signature in polygon (20) has a high agreement with the Teak woodland and the Burkea woodland polygons. This is probably due to the narrow strip of evergreen forest and the presence of Mopane and Acacia species on the mainland. The t-values in polygon (20) shows a decrease in all bands (Figure 20), although they are to small to indicate a change.

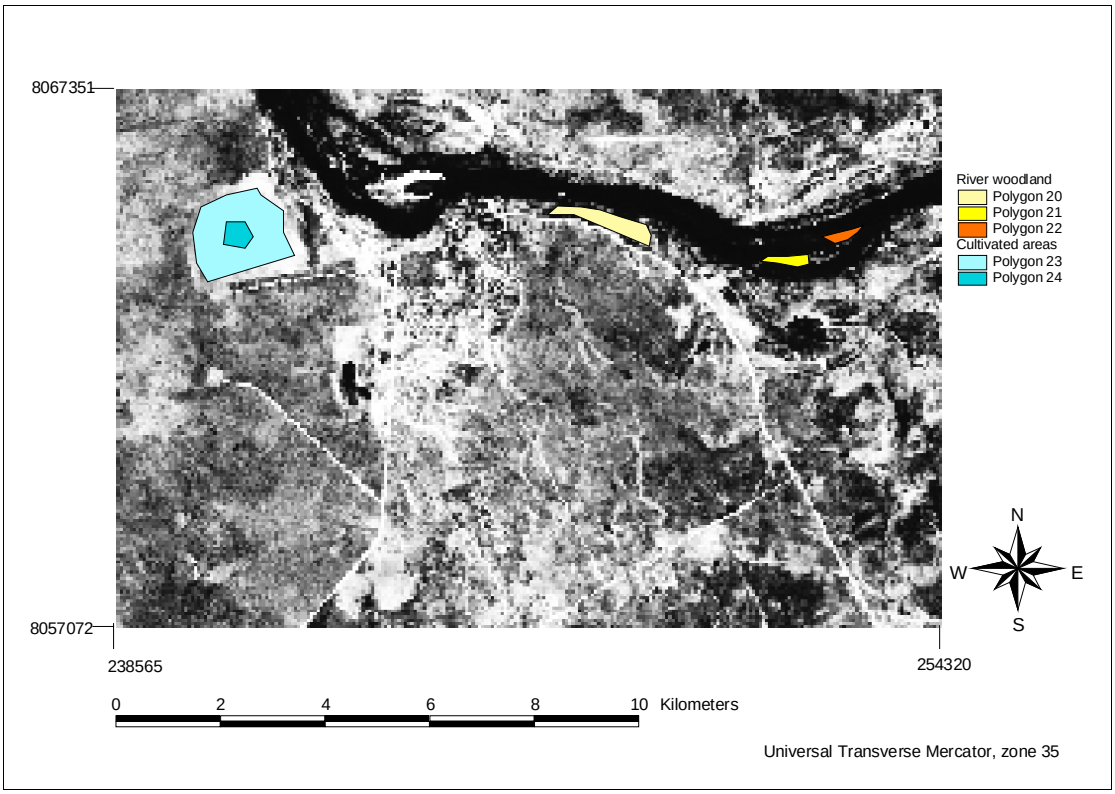

Figure 19. *River woodland in polygons (20) to (22) and cultivated areas in (23) and (24).*

The only band that shows a change according to the t-test is the red band in polygon (21), which indicates a decrease in reflectance (Figure 20). Polygon (21) and (22) are situated on an island in the Zambesi river, which is heavily grassed by cattle. If the vegetation has decreased, the at-satellite reflectance would increase due to a higher soil influence. Also, if the island had expanded during the years, the signature would have increased since soil has a higher reflectance than water. The mean reflectance has decreased in all bands, just like the Teak woodland, except for polygon (21).

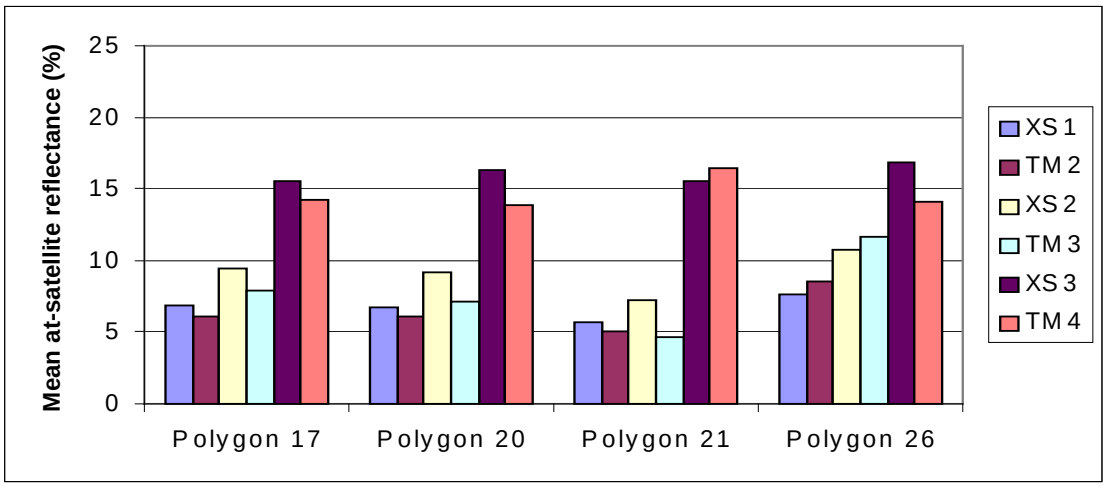

Figure 20. *The mean at-satellite reflectance of Teak woodland polygon (17), river woodland polygon (20) and (21) and the edge of the woodland polygon (26).*

5.4.6 Cultivated areas

Polygon (23) and (24), in cultivated areas (Figure 19), were used since they are situated in a ranch area. Polygon (24) is placed in the middle of an irrigated area while polygon (23) covers the whole cultivation in the TM scenes. It was chosen in order to investigate if the irrigated area had grown during the two years. According to the t-test, no changes have occurred during the period 1992 to 1994. The crop in the irrigated area has recently been harvested and the reflectance of the field is almost the same.

5.4.7 The edge of the wood

The polygon (25), (26) and (27), placed just next to the Teak woodland (Figure 18), shows the same reflectance pattern as shrubland. These areas were chosen since the border between the Teak woodland and the shrubland was distinct. The mean reflectance has increased in the green and the red band but decreased in the near infrared as in polygon (25) (Figure 20). The t-test indicates that all the area has become drier in 1994 than in 1992.

Analysing the BD measure from 1992, the result shows that polygons (25) to (27) has a similar signature to that of the Teak woodland polygons (17) to (19). In 1994 the signature is very close to that of the shrubland, but also to Burkea woodland although not as evident. This implies that the edge of wood polygons has changed from more woodland like to shrubland like vegetation.

6 DISCUSSION

Since the two scenes were taken by different sensors, there were some difficulties in correcting these to each other. The saturation of the SPOT scene also caused problems. The method used to calibrate the two scenes to each other was modified by the authors and thereby not statistically tested and evaluated. Some pixel values in the SPOT scene may be incorrect because of this, which has been considered during the tests.

The vegetation change detection method using variance analysis of spectral signatures is an attempt to study a method that is easy to use. The purpose is to find out if a vegetation change in a minor area has occurred, not having to classify the scenes and create thematic maps. The method proved to be usable, but some problems occurred. It was sometimes difficult to establish the new land cover type if a change had occurred, since some signatures were unseparable according to the BD measure. The Burkea woodland was difficult to separate both from the Teak woodland and the shrubland, even though it is a vegetation type of its own.

6.1 Correcting SPOT to Landsat TM

Most methods found in the literature were not considered to be applicable on the SPOT and the Landsat TM scene, as the former scene was saturated. A histogram matching could not be done on the SPOT data since it contained high extreme values in some of the soil and road pixels that caused problems in the matching. This made the histogram of each SPOT band incorrect, since all values are used to make a regression in order to perform a histogram match.

Both the standardisation and the normalisation methods are only a first order correction and since relevant meteorological and atmospherical data and values of background reflectance were not available, it was impossible to accomplish an absolute atmospheric correction (Hall-Könyves, 1988). In order to use a standardisation method suggested by Hall-Könyves (1988), pixels of low values and high values should be used. Since the SPOT scene contained some high extreme values in the soil, these could not be used in the calculation. Instead woodland and open grassland were used. The results showed that the saturation of the SPOT scene made the standardisation method not suitable. The difference after the transformation between pixel values of stable areas was unacceptable.

The method used was a combination of the normalisation method and the relative calibration. The Landsat TM scene was used as standard since it proved to be the most reliable (e.g. it was normally distributed and without extreme values). Instead of using raw data, suggested by Muller (1993), the scene was radiometrically corrected to at-satellite reflectance. This was done in order to correct for scene and sensor related effects, and to minimise errors caused by these effects in the following analysis of the spectral signature. Thirty values were chosen and a regression equation was calculated and applied on the SPOT scene.

6.2 Fourier analysis

The Fourier analysis showed that the two scenes were taken at approximately the same phenological time. The 10 day composites were combined two and two to 20 day composites since the cloud contamination of the NOAA NDVI scenes influenced the calculations. A 30 day composite would give an even better noise reduction, but the accuracy that ought to be obtained would be lost. The approximative day of decrease in 1992 and 1994, 2/4 and 16/4 respectively, lies in the same phenological period of time that makes them comparable according to spectral signature.

The Fourier program is very sensitive for cloud coverage in the image, which affects the results. Visual studies of the images implied that this was not a major problem in this case since the study area was relatively cloud free during the period 1991-1994.

6.3 Vegetation change analysis

Using a variance analysis on two satellite scenes, in order to establish if any land cover changes have occurred, proved to be useful. Only a few changes were established and most of them indicated a drier climate, which is verified by climate data from the area. Unfortunately, the results from the SPOT bands could not be properly evaluated due to lack of spectral resolution. The SPOT data turned out to be less useful than the Landsat TM as it was saturated which made the raw digital number range more narrow than preferred. The DN values of the SPOT scenes were corrected to the TM scene, but their internal relation were not altered.

When analysing the resulting t-values, a relatively high value was chosen in order to reject the H_0 hypothesis. Some changes in the reflectance values might be due to the normalisation method and another error may be caused by the use of different sensors and the fact that the SPOT scene was saturated. Choosing a high t-value would minimise a false change, resulting from errors caused by the normalisation method and the saturation. The Vegetation Map (1997) was used as evaluation, since it was based on the 1994 Landsat TM scene and had been properly examined with field studies. The lack of details in the map, such as no fire scars or cultivated areas were present, caused some problems. The field study carried out by the authors, discussions with the NRSC and conversation with locals were used to establish the fire areas and the cultivated ranch area.

As expected, the changes of the vegetation were small which depends on the short time period. Over all, the spectral signatures implied drier conditions during the years. The years 1991 to 1998 has been unusually dry in the Caprivi area and hence, the amount of green vegetation has decreased. Polygon (3), consisting of open grassland, is most likely influenced by humans trying to cultivate the area. Polygon (4) may have been cultivated in 1992 but then abandoned before 1994 as it then consists of grassland. The BD measure implies that the change in (4) also could have been caused by drought, as the reflectance in 1992 also is similar to that of shrubland.

The shrubland and the edge of the woodland are most likely influenced by drought. It is also possible that the edge of the woodland polygons has suffered a combination of drought and human logging. The Battacharrya separability analysis implies that the vegetation by the edge of the woodland has changed from Teak woodland to shrubland.

The change of the at-satellite reflectance in the Teak woodland is difficult to explain. The signature decrease in all three bands could not be explained by drought only since a higher amount of senesced vegetation would give an increase in the green and the red band, but a decrease in the near infrared. The decrease in all bands also occur in river woodland and may be due to the fact that these two woodlands consist of more evergreen species than the other land cover types. Literature studies could not explain the phenomena.

The fact that the polygons in the Burkea woodland show no changes at all, while the Teak woodland and the shrubland has changed is probably due to the different species in the two land cover types. Analyses made by Elvidge (1990) concluded that the reflectance of stems and branches of Burkea and Teak species differ from each other. If the stems affected the signature in 1994 in a higher degree than in 1992, the reflectance would have increased. The Burkea stem has a reddish colour, while the Teak stem colour is greyer (van Wyk & van Wyk, 1995). This affects the spectral reflectance when the leaves senesces and falls as the reflectance spectra of red stem is higher than that of grey stem (Figure 21).

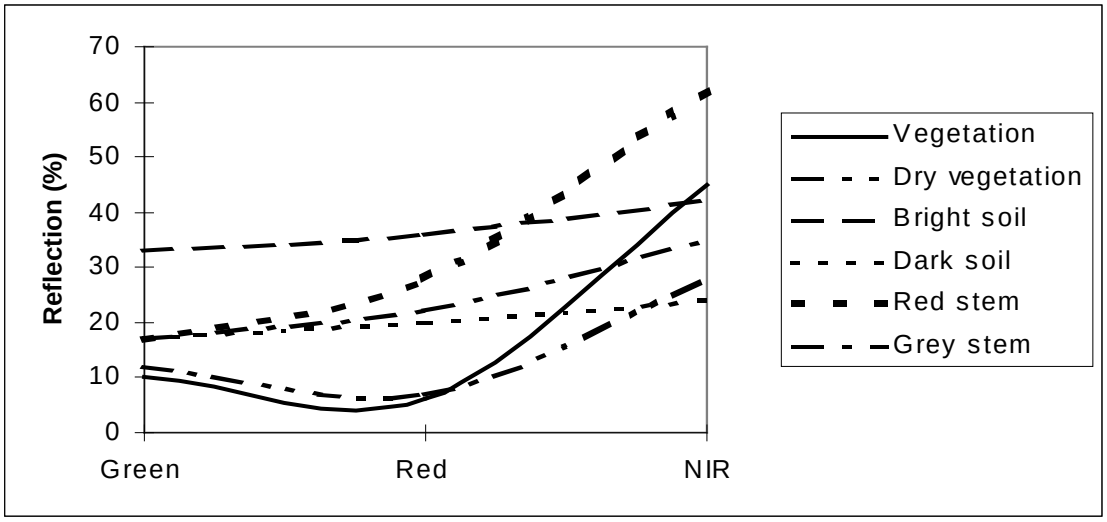

Figure 21. *The reflectance spectra of red and grey stem, bright and dark soil, vegetation and dry vegetation (Elvidge, 1990; Ringrose et al, 1989). The standard deviations of the red and grey stem signatures are not known.*

The unnoticeable change in the Burkea woodland may also depend on that the senesced vegetation and the soil in 1994 gives a reflectance close to that in 1992. Most likely, the drought has influenced the Burkea woodland just as the other shrubland and woodlands, but does not show as much.

The results of the variance analysis using t-test indicates it is a method that is worth continued research. The difficulties lies in the problems to interpret the spectral

differences in the bands used. However, this study has shown that the use of a variance test in order to find out if there had been any changes in the vegetation has proved to be reliable in combination with a signature separability analysis. A more pronounced result could be achieved when using a longer time period. In this study, the period was only two years and the only changes that were distinct was the fire scars. Also, scenes from the same satellite, preferrably Landsat TM, would enhance the results since Landsat TM gives a better result when analysing vegetation than does SPOT. The SPOT sensor is often saturated and therefore not reliable according to signatures.

7 CONCLUSIONS

The normalisation method used on the SPOT scene corrected the pixel values and made them comparable to those in the relative calibrated Landsat TM scene. The method, using the mean pixel value of stable areas, proved to be the most fitting in this study, since the SPOT scene was saturated. This made it inappropriate to use methods based on stable areas such as soil.

Using a vegetation change method based on a variance analysis turned out to be useful. The paired t-test showed that only minor changes has occurred during the time period 1992 to 1994, which was expected.

The study area in Caprivi has not experienced any extensive change between 1992 and 1994. The changes detected are mainly due to drought and fires, although some areas in the open grassland and grassland has been cultivated by humans. The paired t-test and the Battacharrya separability analysis showed changes in almost all land cover classes, although they sometimes were small.

The variance analysis is a suitable tool in detecting land cover changes when combined with the Battacharrya separability analysis, but further investigations are needed.

8 REFERENCES

Ahlcrona, E., 1988. *The Impact on Land Transformation in Central Sudan, Application of Remote Sensing,* Meddelanden från Lunds Universitets Geografiska Institutioner, avhandlingar 103, Lund.

Bond, W. J., 1997. *Fire*, Vegetation of Southern Africa, edited by Cowling, R. M., Richardson, D. M. and Pierce, S. M., Cambridge University Press, Cambridge. (kap 18).

Büttner, G. & Csillag, F., 1989. Comparative Study of Crop and Soil Mapping Using Multitemporal and Multispectral SPOT and Landsat Thematic Mapper Data, *Remote Sens. Environ.*, (vol 29) 3: 241 - 249.

Campbell, J. B., 1996. *Introduction to Remote Sensing*, 3rd edition. Taylor & Francis Ltd, London.

Cowling, R. M. and Hilton-Taylor, C., 1997. *Phytogeography, flora and endemism*, Vegetation of Southern Africa, edited by Cowling, R. M., Richardson, D. M. and Pierce, S. M., Cambridge University Press, Cambridge.

Dadhwal, V. K., Parihar, J. S., Medhavy, T. T., Ruhal, D. S., Jarwal, S. D. & Khera, A. P., 1996. Comparative performance of thematic mapper middle-infraredbands in crop descrimination, *Int. J. Remote Sensing*, (vol 17) 9:1727-1734.

DCW, 1992. *Digital Chart of the World*, 1st edition, Defence Map Agency, USA.

Eastman, J. R., 1993. *IDRISI Version 4.1, Update Manual*, Clark University, Graduate School of Geography, Worcester.

Eklundh, L., 1996. *AVHRR NDVI for monitoring and mapping of vegetation and drought in East African environments*, Meddelanden från Lunds Universitets Geografiska Institutioner, avhandlingar 126, Lund.

Elvidge, C. D., 1990. Visible and near infrared characteristics of dry plant materials, *Int. J. Remote Sensing*, 11:1775-1795.

esa, 1991. *Report of the earth observation user consulation meeting*, esa sp-1143 october 1991, ESTEC, Noordwijk.

ESRI, 1996. *Arc View GIS Version 3.0, Using Arc View GIS*, ESRI Inc, Washington DC.

Guyot, G. & Gu, X-F., 1994. Effect of Radiometric Corrections on NDVI-Determined from SPOT-HRV and Landsat-TM data, *Remote Sens. Environ.*, (vol 49) 3:169-180.

Hall-Könyves, K., 1988. *Remote Sensing of Cultivated Lands in the South of Sweden*, Meddelanden från Lunds Universitets Geografiska Institutioner, Avhandlingar 102, University of Lund, Lund.

Henebry, G. M., 1993. Detecting changes in grasslands using measures of spatial dependence with Landsat TM data. *Remote Sens. Environ.*, (vol 46) 2:223-234.

Hill, J. & Aifadopoulou, D., 1990. Comparative Analysis of Landsat-5 TM and SPOT HRV-1 Data for Use in Multiple Sensor Approaches, *Remote Sens. Environ.*, (vol 34) 1:55-70.

Joria, P. E., Ahearn, S. C. & Connor, M., 1991. A Comparison of the SPOT and Landsat Thematic Mapper Satellite Systems for Detecting Gypsy Moth Defoliation in Michigan, *Photogrammetric Engineering & Remote Sensing*, (vol 57) 12: 1605 - 1612.

Kennedy, P. J., 1989. Monitoring the phenology of Tunisian grazing lands, *Int. J. Remote Sensing*, (vol 10) 4-5: 835 - 845.

Lillesand, T. M. & Kiefer, R. W., 1979. *Remote Sensing and Image Interpretation*, 2nd edition. John Wiley & Sons, Inc, New York.

Markham, B. L. & Barker, J. L., 1986. Landsat MSS and TM Post-calibration Dynamic Ranges, Exoatmospheric Reflectance, and At-Satellite Tempratures. *Landsat Technical Notes.* 1:3-8.

Muller, E., 1993. Evaluation and Correction of Angular Anisotropic Effects in Multidate SPOT and Thematic Mapper Data, *Remote Sens. Environ*, (vol 45) 3: 295 - 309.

NRSC, 1998. Unpublished material, NRSC, Namibia.

Olsson, L. & Eklundh, L., 1994. Fourier Series for analysis of temporal sequences of satellite sensor imagery, *Int. J. Remote Sensing*, (vol 15) 18: 3735 - 3741.

PCI, 1994. *Using PCI Software, Version 5.3 EASI/PACE*, PCI Inc., Richmond Hill.

Pereira, M. C. & Setzer, A. W., 1993. Spectral characteristics of fire scares in Landsat-5 TM images of Amazonia, *Int. J. Remote Sensing*, (vol 14) 11:2061-2078

Pilesjö, P., 1992. *GIS and Remote Sensing for Soil Erosion Studies in Semi-arid Environments*, Meddelanden från Lunds Universitet, Avhandlingar 114, University of Lund, Lund.

Price, J. C., 1987. Calibration of Satellite Radiometers and the Comparison of Vegetation Indices, *Remote Sens. Environ.*, (vol 21) 1: 15 - 27.

Richards, J. A., 1986. *Remote Sensing Digital Image Analysis*, 2nd edition. Springer-Verlag, New York.

Ringrose, S., Matheson, W., Mgotsi, B. & Tempset, F., 1989. The Darkening Effect in Drought Affected Savanna Woodland Environments Relative to Soil Reflectance in Landsat and SPOT Wavebands, *Remote Sens. Environ.*, (vol 30) 1:1-19

Ringrose, S., Vanderpost, C. & Matheson, W., 1997. Use of image processing and GIS techniques to determine the extent and possible causes of land management/fenceline induced degradation problems in the Okavango area, northern Botswana, *Remote Sens. Environ.*, (vol 18) 11:2337-2346.

Scholes, R. J., 1997. *Savanna*, Vegetation of Southern Africa, edited by Cowling, R. M., Richardson, D. M. and Pierce, S. M., Cambridge University Press, Cambridge.

Schott, J. R., 1997. *Remote Sensing: The Image Chain Approach*, Oxford University Press, Inc, New York.

Schulze, R. E., 1997. *Climate*, Vegetation of Southern Africa, edited by Cowling, R. M., Richardson, D. M. and Pierce, S. M., Cambridge University Press, Cambridge.

Shaw, G. & Wheeler, D., 1994. *Statistical Techniques in Geographical Analysis*, 2nd edition, David Fulton Publishers, London.

Tucker, C. J., 1979. Red and photographic infrared linear combinations for monitoring vegetation, *Remote Sens. Environ.*, 8: 127 - 150.

Williamson, H. D. & Eldridge, D. J., 1993. Pasture statues in semi-arid grassland, *Int. J. Remote Sensing*, (vol 14) 13:2535-2546

Windhoek Weather Bureau, 1997. Private Bag 13226, Windhoek.

van Wyk, B. & van Wyk, P., 1995. *Field guide to trees of southern Africa*, Struik Publishers Ltd, Cape Town.

Maps:
ONC P-4, 1989. *Elevation map*, 4th ed, Defense Mapping Agency Aerospace Center, St. Louis, USA.
Soil Map, 1997. *The soils in the Caprivi area,* NRSC, Namibia.
Vegetation map, 1997. *The vegetation in Caprivi*, NRSC, Namibia.

8.1.1

8.1.2 APPENDICES

8.2 Appendix I

The result of the Battacharrya separability analysis on SPOT XS.

Polygon	1	2	3	4	5	6	7	8	9	10	11	12	13	14	15	16	17	18	19	20
2	1.89																			
3	0.32	1.65																		
4	1.66	1.38	1.29																	
5	1.99	1.95	1.92	1.81																
6	1.99	1.91	1.91	1.66	0.07															
7	1.88	1.77	1.61	0.63	1.18	0.99														
8	1.88	1.3	1.56	0.57	1.31	1.12	0.37													
9	2	1.99	1.97	1.84	0.57	0.51	1.26	1.61												
10	2	2	1.98	1.85	1.01	0.92	1.21	1.68	0.22											
11	1.99	1.84	1.87	1.72	0.22	0.3	1.19	1.09	1.1	1.47										
12	1.86	1.2	1.53	1.03	0.69	0.7	0.8	0.4	1.39	1.64	0.43									
13	1.87	1.12	1.58	1.17	0.73	0.77	1.03	0.56	1.48	1.75	0.43	0.05								
14	1.85	0.83	1.54	1.34	1.15	1.21	1.43	0.91	1.75	1.93	0.72	0.31	0.19							
15	1.64	0.78	1.27	1.06	1.31	1.34	1.36	0.86	1.79	1.93	0.96	0.41	0.31	0.11						
16	1.81	0.98	1.47	0.95	0.81	0.78	0.98	0.45	1.48	1.75	0.53	0.07	0.07	0.25	0.29					
17	1.98	1.76	1.86	1.75	0.33	0.44	1.19	1.02	1.15	1.49	0.11	0.38	0.36	0.65	0.89	0.53				
18	1.99	1.91	1.92	1.96	0.54	0.74	1.69	1.58	1.43	1.78	0.22	0.78	0.74	0.84	1.1	0.84	0.35			
19	1.99	1.89	1.91	1.95	0.77	0.98	1.71	1.56	1.62	1.88	0.3	0.77	0.71	0.72	1	0.86	0.37	0.11		
20	1.88	1.31	1.62	1.26	0.59	0.63	0.93	0.77	1.08	1.34	0.48	0.22	0.23	0.44	0.54	0.31	0.45	0.78	0.79	
21	1.84	1.59	1.64	1.53	1.32	1.32	1.34	1.36	1.45	1.55	1.2	1.06	1.09	1.07	1.11	1.11	1.22	1.29	1.25	0.85
22	1.86	1.64	1.66	1.34	1.33	1.22	1.36	1.24	1.64	1.48	1.22	0.92	0.85	1.02	0.99	0.84	1.20	1.08	1.32	0.42
23	1.37	1.43	0.82	0.56	1.32	1.24	0.53	0.56	1.51	1.54	1.26	0.66	0.87	1.09	0.9	0.72	1.24	1.56	1.58	0.85
24	1.38	1.49	0.86	0.66	1.42	1.29	0.52	0.59	1.52	1.57	1.28	0.59	0.92	1.02	0.92	0.72	1.21	1.55	1.65	0.87
25	1.87	1.45	1.54	0.93	0.7	0.67	0.49	0.28	1.24	1.42	0.6	0.12	0.28	0.71	0.74	0.3	0.51	1.05	1.08	0.34
26	1.91	1.11	1.63	1.19	0.88	0.87	0.95	0.47	1.55	1.74	0.45	0.14	0.14	0.26	0.42	0.18	0.33	0.7	0.61	0.4
27	1.74	1.18	1.35	0.38	1.24	1.11	0.34	0.13	1.57	1.66	1.04	0.36	0.47	0.74	0.64	0.39	0.95	1.45	1.42	0.65

The result of the Battacharrya separability analysis on Landsat TM.

Polygon	1	2	3	4	5	6	7	8	9	10	11	12	13	14	15	16	17	18	19	20	21
2	0.83																				
3	1.11	1.13																			
4	1.3	1.38	1.35																		
5	2	2	1.38	1.97																	
6	1.99	2	1.22	1.98	0.39																
7	1.91	1.99	1.24	1.31	1.36	1.51															
8	1.98	2	1.2	1.88	0.22	0.52	0.85														
9	2	2	1.8	2	1.79	1.57	2	1.93													
10	2	2	1.91	2	1.95	1.87	2	1.99	0.72												
11	2	2	1.93	2	1.97	1.84	2	1.99	1.44	0.99											
12	2	2	1.63	2	1.71	1.04	1.95	1.81	1.09	1.57	1.69										
13	2	2	1.89	2	2	1.98	1.99	2	2	2	2	1.21									
14	2	2	1.82	2	2	1.93	1.98	1.99	2	2	2	1.13	0.17								
15	1.99	2	1.72	2	2	1.92	1.97	1.98	2	2	2	1.1	0.16	0.15							
16	2	2	1.9	2	2	1.93	1.99	1.99	1.99	2	1.99	1.09	0.16	0.12	0.29						

17	2	2	2	2	2	1.99	2	2	2	2	1.94	1.93	1.85	1.69	1.8	1.65						
18	2	2	1.99	2	2	1.97	2	2	2	2	1.92	1.86	1.82	1.66	1.76	1.6	0.25					
19	2	2	2	2	2	1.99	2	2	2	2	1.92	1.97	1.94	1.85	1.91	1.84	0.15	0.47				
20	2	2	1.92	2	1.95	1.79	1.99	1.97	1.87	1.89	1.66	1.51	1.67	1.42	1.62	1.41	0.73	0.94	0.73			
21	2	2	1.91	2	1.94	1.86	1.99	1.96	1.75	1.67	1.64	1.74	1.88	1.76	1.85	1.79	1.69	1.78	1.66	0.96		
22	1.99	1.99	1.61	1.99	1.67	1.32	1.89	1.71	1.47	1.59	1.41	0.96	1.37	1.14	1.26	1.16	1.26	1.38	1.3	0.38	0.7	
23	1.6	1.55	0.47	1.66	1.36	1.09	1.43	1.22	1.74	1.86	1.85	1.28	1.6	1.42	1.32	1.6	1.95	1.93	1.96	1.74	1.82	1
24	2	2	0.55	1.75	1.40	1.05	1.44	1.29	1.89	1.91	1.82	1.26	1.62	1.44	1.42	1.62	2	2	2	1.77	1.92	1
25	1.96	1.98	1.14	1.95	0.86	0.48	1.5	0.87	1.59	1.85	1.82	0.7	1.37	1.31	1.24	1.3	1.78	1.67	1.84	1.62	1.84	1
26	1.87	1.97	0.88	1.59	1.14	0.87	0.57	0.67	1.94	1.98	1.95	1.23	1.75	1.6	1.53	1.65	1.86	1.78	1.88	1.7	1.88	1
27	1.6	1.78	0.68	1.12	1.08	1.1	0.32	0.61	1.97	1.99	1.99	1.73	1.9	1.85	1.77	1.9	1.99	1.99	2	1.95	1.96	1

8.3 Appendix II

The mean at-satellite reflectance (%), standard deviation (%) and resulting t-value for each band and polygon.

			9 Mean	10 St Dev	11 T-Value			12 Mean	13 St Dev	14 T-Value
		XS1	11.5	0.10			XS1	8.07	0.72	
15	Poly. 1					16	Poly. 2			
		TM2	11.4	0.54			TM2	10.7	0.75	
		Differ	0.07	0.81			Differ	-2.63	0.91	
					0.53					-38.04
		XS2	16.7	1.58			XS2	11.4	1.01	
		TM3	16.4	0.93			TM3	15.1	1.11	
		Differ	0.34	1.3			Differ	-3.7	1.28	
					1.65					-37.87
		XS3	20.9	1.29			XS3	15.9	1.03	
		TM4	21.2	1.09			TM4	20.4	1.04	
		Differ	-0.29	1.02			Differ	-4.46	1.55	
					-1.74					-37.83
		XS1	10.9	1.30		Poly. 4	XS1	8.86	0.50	
17	Poly. 3									
		TM2	9.7	1.37			TM2	10.4	0.87	
		Differ	1.19	1.43			Differ	-1.60	1.07	
					11.29					-23.17
		XS2	16.0	1.95			XS2	12.4	0.66	
		TM3	13.5	2.33			TM3	14.4	1.05	
		Differ	2.44	2.13			Differ	-2.0	1.34	
					15.56					-23.88
		XS3	20.7	1.76			XS3	18.0	1.03	
		TM4	17.4	3.71			TM4	18.8	0.99	
		Differ	3.32	3.33			Differ	0.83	1.52	
					13.69					-8.6
		XS1	6.9	0.62		Poly. 6	XS1	7.16	0.59	
18	Poly. 5									
		TM2	8.7	0.77			TM2	8.14	0.65	
		Differ	-1.80	0.93			Differ	0.97	0.76	
					-28.58					-26.48
		XS2	9.20	0.73			XS2	9.32	0.73	
		TM3	11.9	1.15			TM3	11.1	0.97	
		Differ	-2.70	1.28			Differ	-1.80	1.04	
					32.24					-35.49
		XS3	16.5	1.22			XS3	17.1	1.19	
		TM4	14.4	1.12			TM4	14.3	1.04	

		Differ	2.02	1.58			Differ	2.80	1.41	
					19.51					41.36

			Mean	StDev	T-value				Mean	StDev	T-value
		XS1	7.94	5.87				XS1	7.91	0.63	
19	**Poly.7**					**20**	**Poly.8**				
		TM2	10.5	0.70				TM2	9.24	0.73	
		Differ	-2.5	0.87				Differ	-1.3	0.86	
					-29.78						-30.54
		XS2	11.0	0.75				XS2	11.0	0.85	
		TM3	14.5	0.86				TM3	12.7	1.00	
		Differ	-0.35	1.18				Differ	-1.70	1.17	
					-30.31						-29.5
		XS3	18.0	1.10				XS3	17.2	1.14	
		TM4	17.4	0.91				TM4	15.3	1.10	
		Differ	0.61	1.44				Differ	1.81	1.30	
					4.33						27.53
		XS1	7.29	0.55		**Poly.10**		XS1	7.18	0.45	
21	**Poly.9**										
		TM2	6.93	0.35				TM2	6.41	0.32	
		Differ	0.36	0.61				Differ	0.77	0.55	
					6.82						8.74
		XS2	9.38	0.61				XS2	9.47	0.56	
		TM3	8.86	0.52				TM3	7.99	0.62	
		Differ	0.52	0.71				Differ	1.47	0.83	
					8.56						11.05
		XS3	18.5	1.15				XS3	18.6	1.02	
		TM4	10.5	0.93				TM4	9.32	1.09	
		Differ	7.96	1.47				Differ	9.25	1.52	
					63.21						37.85
Poly.11		XS1	7.38	0.66				XS1	7.76	1.17	
						22	**Poly.12**				
		TM2	6.89	0.45				TM2	7.89	0.35	
		Differ	0.49	0.65				Differ	0.14	1.14	
					6.16						-1.5
		XS2	9.85	0.74				XS2	10.9	1.68	
		TM3	8.77	0.72				TM3	11.0	0.61	
		Differ	1.08	0.82				Differ	-0.16	1.62	
					10.6						-1.26
		XS3	17.5	1.33				XS3	16.6	1.25	
		TM4	10.6	0.97				TM4	17.1	0.89	
		Differ	6.95	1.16				Differ	-0.44	1.41	

				48.62					-3.87
		XS1	7.19	1.04			XS1	7.69	1.30
23	**Poly.13**				**24**	**Poly.14**			
		TM2	7.50	0.40			TM2	7.51	0.53
		Differ	-0.31	1.04			Differ	0.18	1.33
				-4.5					1.23
		XS2	9.89	1.41			XS2	10.5	1.72
		TM3	10.4	0.66			TM3	10.1	0.78
		Differ	-0.49	1.43			Differ	0.43	1.75
				-5.2					2.91
		XS3	15.9	1.05			XS3	15.6	1.14
		TM4	16.7	0.76			TM4	16.2	0.87
		Differ	-0.81	1.18			Differ	-0.67	1.45
				-10.48					-5.4
			Mean	**StDev**	**T-value**			**Mean**	**StDev**	**T-value**
		XS1	7.68	1.33			XS1	8.10	1.36	
25	**Poly.15**				**26**	**Poly.16**				
		TM2	7.41	0.45			TM2	7.61	0.60	
		Differ	0.27	1.32			Differ	0.47	1.20	
				2.38					3.91	
		XS2	10.5	1.91			XS2	11.2	2.12	
		TM3	10.0	0.68			TM3	10.4	0.83	
		Differ	0.53	1.89			Differ	0.81	1.86	
				3.17					4.4	
		XS3	15.8	1.11			XS3	16.2	1.44	
		TM4	16.4	0.99			TM4	16.4	0.97	
		Differ	-0.58	1.51			Differ	-0.19	1.38	
				-4.41					-1.41	
		XS1	6.85	0.64			XS1	6.51	0.42	
27	**Poly.17**				**28**	**Poly.18**				
		TM2	6.05	0.63			TM2	6.10	0.30	
		Differ	0.80	0.81			Differ	0.41	0.48	
				15.54					12.91	
		XS2	9.40	0.78			XS2	8.65	0.54	
		TM3	7.95	0.57			TM3	7.99	0.55	
		Differ	1.44	0.92			Differ	0.66	0.72	
				24.97					13.84	
		XS3	15.6	1.10			XS3	14.8	1.10	
		TM4	14.2	0.92			TM4	14.1	0.76	
		Differ	1.40	1.34			Differ	0.73	1.35	
				16.55					8.14	
		XS1	6.18	0.44		**Poly.20**	XS1	6.75	1.30	
29	**Poly.19**									
		TM2	5.72	0.33			TM2	6.07	0.63	
		Differ	0.46	0.52			Differ	0.69	1.17	

				14.04					4.49
	XS2	8.16	0.57			XS2	9.22	1.98	
	TM3	7.11	0.57			TM3	7.16	1.11	
	Differ	1.06	0.73			Differ	2.05	1.63	
				22.83					9.57
	XS3	14.6	1.13			XS3	16.3	2.08	
	TM4	13.7	1.76			TM4	13.8	1.65	
	Differ	0.98	2.11			Differ	2.45	2.46	
				7.41					7.57
Poly.21	XS1	5.76	0.34		**Poly.22**	XS1	6.89	2.25	
	TM2	5.11	0.36			TM2	5.65	0.84	
	Differ	0.64	0.48			Differ	1.23	2.02	
				4.96					2.79
	XS2	7.23	0.46			XS2	9.34	3.45	
	TM3	4.67	0.27			TM3	5.67	1.79	
	Differ	2.55	0.49			Differ	3.67	3.11	
				19.49					5.39
	XS3	15.5	1.51			XS3	15.9	2.05	
	TM4	16.5	2.76			TM4	14.7	1.63	
	Differ	-1.0	1.72			Differ	1.22	2.25	
				-2.2					2.49
		Mean	**StDev**	**T-value**			**Mean**	**StDev**	**T-value**
Poly.23	XS1	8.47	0.97		**Poly.24**	XS1	8.67	0.83	
	TM2	9.05	1.12			TM2	9.22	1.12	
	Differ	-0.58	1.09			Differ	-0.54	1.12	
				-12.83					-4.36
	XS2	12.2	1.61			XS2	12.8	1.48	
	TM3	12.6	1.76			TM3	13.1	2.12	
	Differ	-0.39	1.80			Differ	-0.36	1.90	
				-5.35					-1.71
	XS3	18.2	1.43			XS3	18.6	1.52	
	TM4	17.4	2.96			TM4	17.5	2.50	
	Differ	0.77	2.77			Differ	1.12	2.58	
				6.81					3.9
	XS1	7.62	0.54			XS1	7.32	0.75	
30	**Poly.25**				**31**	**Poly.26**			
	TM2	8.59	0.55			TM2	9.47	1.07	
	Differ	-0.97	0.69			Differ	-2.15	1.05	
				-18.37					-19.81
	XS2	10.7	0.78			XS2	9.98	0.95	
	TM3	11.7	0.91			TM3	13.1	1.51	
	Differ	-0.10	0.95			Differ	-3.12	1.36	
				-12.85					-22.14
	XS3	16.8	0.81			XS3	15.7	1.21	
	TM4	14.1	1.64			TM4	16.6	1.22	
	Differ	2.72	1.77			Differ	-0.89	1.40	
				20.16					-6.14

		XS1	8.17	0.88	
32	**Poly.27**				
		TM2	9.54	1.02	
		Differ	-1.37	1.17	
					-14.07
		XS2	11.3	1.08	
		TM3	13.4	1.40	
		Differ	-2.06	1.55	
					-15.97
		XS3	17.3	1.52	
		TM4	16.7	1.43	
		Differ	0.48	1.82	
					3.18

32.1 Appendix III

The mean at-satellite reflectance (%) in the green, red and near infrared band of polygons (1) to (27).